Article

Not peer-reviewed version

Optimization of Silver Nanoparticle Coating Methods on Acrylic, Silicone, and Zirconia Facial Prosthetic Materials: Surface Characterization and Antimicrobial Activity Against *Pseudomonas aeruginosa*

Wan Mand Dizayee *, Zhala Dara Omer Meran , Layla A. Abu-Naba'a

Posted Date: 6 May 2026

doi: 10.20944/preprints202605.0288.v1

Keywords: PMMA; maxillofacial silicone; zirconium; Ag nanoparticle; coating method; *Pseudomonas aeruginosa*; spray coating; adhesion test; direct contact test

 doi:10.20944/preprints202605.0288.v1

Article

Optimization of Silver Nanoparticle Coating Methods on Acrylic, Silicone, and Zirconia Facial Prosthetic Materials: Surface Characterization and Antimicrobial Activity Against *Pseudomonas aeruginosa*

Wan Mand Dizayee [1,*], Zhala Dara Omer Meran [1] and Layla A. Abu-Naba'a [2]

[1] Department of Prosthodontics, College of Dentistry, Hawler Medical University, Erbil 44001, Kurdistan Region, Iraq

[2] Department of Prosthodontics, Jordan University of Science and Technology, Irbid, Jordan

* Correspondence: wan.mand@den.hmu.edu.krd

Abstract

Background/Objectives: One of the ongoing clinical constraints is limiting microbial growth on facial and dental prostheses, justifying the need for material surface enhancements for reducing the associated microbial complications. This study aimed to investigate a clinically applicable and reproducible coating technique to overcome microbial clinical challenges. **Methods**: Ag nanoparticles (NPs) were applied to three types of facial materials through spray, spin, and dip coating techniques. Surface characterization, elemental composition, and chemical bond formation were assessed by Scanning Electron Microscopy (SEM), Energy-dispersive X-ray Spectroscopy (EDS), and Fourier Transform Infrared (FTIR) spectroscopy, respectively. Subsequent optimization of spray numbers was performed. Antimicrobial performance was examined by agar diffusion, direct contact, and adhesion (time-dependent) assays, with different layers, against *Pseudomonas aeruginosa*. **Results**: Spray coating exhibited superior coating uniformity compared with others. 15 sprays was determined as optimal number for a single layer coating. EDS confirmed Ag NP presence, FTIR revealed no chemical alteration of specimens. Disk diffusion tests showed no inhibition zones. Adhesion and direct contact tests displayed antibacterial activity, the effect of which was stronger for the latter. Time-dependent adhesion test of 1-layer coating of acrylic and silicone had a consistent decrease in bacterial amount, whilst zirconia had only a strong initial activity. In general, the 3-layer coating did not showcase an increased antimicrobial activity, suggesting that the increase in layering negatively impacts surface effectiveness. **Conclusions**: spray coating of Ag NPs can provide a promising, clinically-applicable, large-scale manufacturing strategy for improving dental and facial material antibacterial qualities without altering the inherent prosthetic properties.

Keywords: PMMA; maxillofacial silicone; zirconium; Ag nanoparticle; coating method; *Pseudomonas aeruginosa;* spray coating; adhesion test; direct contact test

1. Introduction

Acrylic resin, Silicone, and Zirconium are widely used facial materials. The broad application of acrylic resins, most commonly polymethyl methacrylate (PMMA), in prosthodontics, orthodontics, and maxillofacial prosthetics is associated with their beneficial qualities of cost-effectiveness, ease of fabrication, and esthetic appeal [1]. Silicone elastomers too have exceptional physical and chemical properties and thus are the most preferred material for extraoral prostheses and are frequently utilized alongside PMMA [2].

 doi:10.20944/preprints202605.0288.v1

However, a considerable disadvantage of Silicone as prostheses, is its susceptibility to colonization by microbes, which may be due to morphological changes of the facial tissues owing to the lesion, and the resulting disturbance in the balance of microbial flora. Acrylic resins share this disadvantage and may cause denture stomatitis and secondary carries [2,3]. As a result, infection is a considerable complication in both silicone and PMMA prosthetics [4].

Additionally, whilst Computer-aided design/computer-aided manufacturing (CAD/CAM)-utilized Zirconium-based restorations have shown higher biocompatibility, fewer microbial adhesions and biofilm formation and, as a result, are less harmful to the periodontal tissues, they are still considerably susceptible to microbial adhesion and the associated complications [5].

Biofilm is a three-dimensional matrix formed from insoluble gelatinous exopolymers released by microbes that adhere to surfaces, and is of significance for patients because they are hard to treat and may result in chronic or recurrent conditions; since biofilms are inherently more resistant to the host's immune system, topical treatments, and antibiotics [2,6].

Methods to reduce biofilm on dentures include brushing and use of cleanser agents, and both are needed for an effective result. However, the use of cleansing agents can damage the denture and harmfully alter its physical and chemical properties [7,8].

This bring us to nanoparticles (NPs), which are utilized for their many beneficial enhancements, including the increase of antimicrobial properties by disruption of biofilm formation and thus, reducing microbial adhesions [1].

Ag is widely known for its antimicrobial activity, especially when utilized as NPs. Natarajan et al. showed that AgNPs are among the NPs with the highest antimicrobial action. AgNPs possess a large surface area to volume ratio, giving it particular properties which substantially increase its antimicrobial effects [1]. The mechanisms of antibacterial effects of AgNPs are primarily through morphological alterations and deformations, damaging bacterial cell walls. Or through the formation and release of free radicals that have powerful bactericidal effects. However, because they are metal NP, AgNPs are considered toxic in large amounts to eukaryotic human cells, and excess usage might also lead to environmental pollution [6,9].

While these antimicrobial efficiencies are highly important, they demand to concentrate on biocompatibility avoiding cytotoxicity. Standard safety level regarding host is the fundamental requirement for the antimicrobial surface for prolonged contact with oral mucosa. Ag NPs' cytotoxic ability had been aestheticized and might not be ignored in clinical application. Generated Ag ions have toxic effects on mammals' tissues by mechanisms that substantially move parallel with killing of bacteria, such effects is indicated in transport disruption of mitochondrial electron, reactive oxygen species' generation, regardless of intervention with intracellular ion homeostasis [10]. Mentioned effects are assessed as of high concentration-dependent: studies of type vitro dose-response studies having processing human fibroblast , epithelial, and osteoblast cell lines uniformly indicate cell viability loss when concentrations of silver ion exceed the range 1 to 5 mg/L, however viability of cells generally stay above 80% at concentrations at or below 0.1 mg/L [10,11]. Both WHO and the US Environmental Protection Agency have considered 0.1 mg/L as a guideline threshold for accepting concentration of Silver in potable water, providing a global referenced benchmark for systemic silver exposure [12]. Clinical safety arguments for AgNP-based prosthetic coating depends critically on the release profile of the specific configuration used. Colloidal AgNP freely dispersed formulations dispense silver ions continuously into surrounding environment, bulk concentrations generated might approach or exceed cytotoxic thresholds for high loading. Surface-immobilized AgNP systems follow a mechanism of contact-killing, in contrast, normally releasing less than 1 to 2% of total deposited silver into medium surroundings, yielding bulk ion concentrations under those concentrations associated with mammalian cytotoxicity in published researches [13]. Such conditions clearly address that lethal effect is spatially confined to the nanoparticle-bacterial cell interface and despite relying on silver ion accumulation in surrounding medium, causing limitation of potential exposure of adjacent host tissues

 doi:10.20944/preprints202605.0288.v1

Moreover, due to the advantages of time- and cost-effectiveness, ease of procedures, large scale manufacturing, and possibility of impurities, commercial Ag NPs were favorably selected over biosynthesized NPs [14,15].

Among other bacteria, *Pseudomonas aeruginosa* is one of the most frequent microorganism recovered from prostheses, and is commonly associated with pneumonia in hospitalized or institutionalized patients [2]. Additionally, *P. aeruginosa* is one of the three highly multi-drug-resistant microbes in the world, as indicated by WHO, for which new antibiotics is critical [16,17].

There are many methods to utilize AgNPs for improving the antibacterial effects against *P. aeruginosa*. However, methods that involved mixing of AgNPs and the mentioned facial materials have been omitted, since they can alter the mechanical properties of the materials and this study aimed to evaluate antimicrobial properties with preservation of the mechanical properties of the materials [18].

A variety of Ag NP coating methods are present in the literature. However, the present study uses the conventional wet-deposition methods (spray, spin, and dip) due to their ease of operation, cost-effectiveness, ambient processing conditions, clinical translatability to various surface geometries, scalability, and previous experience and use for antimicrobial coating of biomedical devices [19–21]. Additionally, the optimal parameters for these conventional coating methods are yet to be determined [22].

Therefore, the aim of this study is to evaluate the antimicrobial effect of AgNP coatings on the mentioned facial materials against *P. aeruginosa* and to determine the optimal coating technique amongst spray, spin, and dip coating.

2. Materials and Methods

2.1. Preparation of Samples

Disk-shaped specimens with a size of 10mm diameter × 2mm thickness were used for testing all three types of materials (Silicone, Acrylic, Zirconium). The details of the facial materials used are provided in Table 1.

Table 1. Details of the utilized facial materials.

	Trade Name	Manufacturing Details	Key Specifications
Silicone	TeKSil 25 Part A base TeKSil 25 Part B catalyst	Technovent Ltd., Bridgend, UK; Batch No. B24E	Shore A 24, isostatic
Acrylic	Akrodent (shade 30)	Koca Kimya ve Dental Ltd. Şti. (Ankara, Turkey)	Polymethyl Methacrylate (PMMA)-based, Heat-cured
Zirconium	VIVID ST (HT4)	Bristol Computer-aided design/computer-aided manufacturing (CAD/CAM) (Bristol, UK)	High Translucency, isostatic pressed

The silicone was prepared per manufacturer's instructions; the base and the catalyst at a 9:1 ratio by weight were mixed via Renfert twister device at 150 rpm for 5 minutes to ensure a homogenous, bubble-free blend. The specific specimen shape was achieved by placing the blend in a plastic mold created by Computer Numerical Control (CNC) a plasma machine for 24 hours at room temperature. Table A1 (appendix A) contains the details of the general materials and devices used.

Zirconia specimens were designed using Rodin (Gen 2, v1.3; Pac-Dent, Inc., Brea, CA, USA) and Blender (v.4.43; Blender Foundation, Amsterdam, Netherlands) and were subsequently verified using Exocad Dental DB (v3.2 Elefant; Exocad GmbH, Elefsina, Greece). The Zirconia blocks were milled using an open type CAD/CAM milling machine.

Sintering was done in a high temperature furnace that was heated up to 1450-1530°C, where the specimens dwelt for 8 hours, after which they were cooled. The sintered specimens were polished.

 doi:10.20944/preprints202605.0288.v1

Finally, ultrasonic cleaning of the specimens in distilled water and ethanol was performed. After drying, it was followed by the application of a glaze paste and firing at 850°C.

Heat-cured PMMA specimens were fabricated using the conventional lost-wax technique. Wax patterns (10mm × 2mm) were invested in dental flasks. Afterwards, the heat-cured resin was proportioned at a powder-to-liquid ratio of 2.1g:1mL. The material was mixed and packed into the mold at the dough stage. Polymerization was performed in a controlled water bath using a long curing cycle: 74°C for 2 hours, followed by a final boil at 100°C for 30 minutes to minimize residual monomer and porosity.

A digital, 150mm stainless steel caliper was used to confirm the 10×2mm dimensions of the prepared specimens. The details of the sample size prepared and used for the current study are mentioned in Table B2 in appendix B.

2.2. NP Preparation

Commercially available spherical Ag NPs (20nm, 99.99% purity, US Research Nanomaterials, Inc.) were used (see Table A2 in the appendix).

Field Emission Scanning Electron Microscope (FESEM) was performed.

A suspension was prepared at a concentration of 10 mg/mL (0.01 g/mL) using Type I ultrapure water. For a homogeneous, non-agglomerated dispersion, the suspension was processed using a probe sonicator for 20 minutes. To prevent overheating and potential thermal oxidation of the NPs, the suspension was maintained in an ice bath during the sonication process. All glassware were ultrasonically cleaned and chemically decontaminated with acetone and ethanol prior to use.

2.3. Specimen Preparation and Surface Activation

All the specimens of PMMA, Silicone, and Zirconium were cleaned by incubation in 70% ethanol for a couple of hours and were afterwards rinsed by distilled water for 5 minutes. The specimens were then sonicated first in soap and distilled water, and later in pure distilled water, each for 5 minutes. They were dried using 99.98% nitrogen gas at 10 PSI. The specimens were additionally subjected to atmospheric plasma treatment for 40 seconds to improve AgNP adhesion for a more uniform coating by increasing surface hydrophilicity and lowering surface free energy.

2.4. Ag NP Concentration Selection and Suspension Characterization

2.4.1. Minimal Inhibitory Concentration (MIC)

The methodology by Wiegand, et al. [23] was implemented. The working place was in a Class II BSC; UV light was turned on for 30 min and afterwards the cabinet was disinfected with 70% ethanol.

P. aeruginosa was retrieved from frozen culture vials in laboratory freezer and cultured using sterile wooden sticks in the appropriate agar plates. They were then incubated. The relevant microbiological preparation procedure details are mentioned in Table B1 in the appendix.

The MIC of the prepared AgNP suspension was determined using Mueller-Hinton Broth through broth microdilution method in 96-well plates. The microbial suspension was prepared according to the 0.5 McFarland standard (1×10^8 CFU/ mL) using a Spectrophotometer, device details are in Table A1. It was 0.12 at 625 nm for *P. aeruginosa*; well within the standardized range (0.08-0.13 at 625 nm).

The concentration of *P. aeruginosa* was reduced to 1×10^6 CFU/ mL. The suspensions were made homogenous using a vortex mixer.

Two-fold serial dilution of the prepared AgNPs (10mg/mL) was done. Then, to ensure continuous contact between *P. aeruginosa* and AgNPs, a plate shaker was used, and the wells were placed in an incubator with 150–1200 rpm speed at 37 °C for 16-20 h.

The MIC was defined as the lowest concentration at which there was no visible growth by visual inspection.

 doi:10.20944/preprints202605.0288.v1

2.4.2. Minimal Bactericidal Concentration (MBC)

For the MBC, 25 µL aliquots from the partially clear wells were taken and a tenfold serial dilution (10^{-1} to 10^{-4}) in sterile broth was performed, followed by mixing with a vortex for 15 seconds to ensure homogeneity.

Afterwards, 20 µL of each dilution obtained were cultured on the appropriate agar plates using glass beads for a uniform spread. The plates were incubated at 37 °C for 24 hours.

The microbial concentration (CFU/mL) was calculated according to Equation (1) below:

$$CFU/mL = \frac{Number\ of\ colonies\ \times\ Dilution\ factor}{Volume\ of\ culture\ plated\ (mL)} \quad (1)$$

2.4.3. Characterization of AgNP Suspension

The chosen concentration of AgNP suspension was characterized for stability and size; the Zeta potential, and Dynamic Light Scattering (DLS) particle size analysis were performed.

2.5. Coating Methods

Three coating techniques (spray, dip, spin) were assessed to determine the method that most uniformly distributed the NPs each material require one specimen per method of coating, and one blank sample (n=4). In total. 12 samples were required to determine the better coating method for each material. The relevant procedural details and devices used for each method are shown in Table 2. Zirconium specimens by testing 5 , 10 and 15 sprays per layer, The maximum number of sprays per layer was first determined by visual inspection of color acceptability which was 15 sprays per layer.

Table 2. Devices and procedure details for each coating method.

Coating method	Device details	Procedure details
Spray	Air brush (SP-20X, Sparmax, Taiwan) nozzle size (0.2mm), gravity-feed cup capacity (2mL) Air compressor (AS-18, Ningbo Haosheng Pneumatic Machinery Co., Ltd., China)	Air pressure = 63 PSI 1 layer = 15 consecutive sprays
Dip	Langmuir—Blodgett Trough (KSV NIMA/ Biolin Scientific, Espoo, Finland)	Samples dipped for 5 seconds
Spin	WS-400 series spin coater (Laurell Technologies Corp., North Wales, PA, USA)	1000 rpm for 60 seconds (on one side only)

Each specimen of the three materials were coated with the coating methods separately. All specimens after coating were subjected to Scanning Electron Microscope (SEM) and 3D stereomicroscope with 7–45× magnification.

2.5.1. Selection of Optimum Coating Method

All 12 samples (3 uncoated and 9 coated with 3 methods) were subjected to FESEM used in (Characterization lab, Nanotechnology Institute, Jordan University of Science and Technology, Irbid, Jordan) to determine the most desirable coating technique.

Both Everhart Thornley and Backscattered Electron detectors were utilized for analyzing the coated and uncoated samples under High Vacuum (HiVac) mode (10^{-2}–10^{-4} Pa).

To prevent FESEM image distortion, the samples were covered priorly with thin, uniform conductive gold layer in an Argon vacuum (1×10^{-1} mbar) using a sputter coater (Table A1), with a deposition rate of 4 nm/min and a total thickness of 6–7 nm.

The spray method had the most uniform distribution, and was chosen for subsequent tests.

 doi:10.20944/preprints202605.0288.v1

2.6. Selection of Optimum Number of Layers for Spray Coating

Color acceptability was disregarded in favor of evaluating the antimicrobial effects of the coated specimens.

2.6.1. Adhesion Test

Adhesion test was used to determine the optimum number of sprays per layer for the specimens. Zirconia specimens were chosen for evaluating the optimum among 15, 10, and 5 sprays per layer by subjecting them to a 1-hour adhesion test. The results proved 15 sprays/layer as optimum. Other materials were not tested for determining optimum number of sprays/layers since the coating itself was the variable being tested and the lower numbers in zirconia already showed worse antimicrobial effects.

Uncoated, 1 layer-coated, and 3 layer-coated samples were prepared from each of the 3 materials. The coating of a single layer was considered complete when the specimen exhibited dryness via visual inspection. Both sides of the coated samples were sprayed to ensure dependable results. The uncoated specimens served as control group. The relevant and detailed microbiological material and procedural details are mentioned in Table B1 in appendix.

Cultures were prepared using the appropriate agar plates and incubation at 37 °C overnight. The microbial inoculum was prepared using the appropriate broth according to the 0.5 McFarland standard range. All the prepared specimens were placed separately in 1mL of the microbial inoculum inside sterile plastic tubes, and were incubated for 1 hour.

The disks were then removed and rinsed 3 times with 500 µL of sterile 1X phosphate-buffered saline to remove non-adherent microbes. The bacteria remaining on the specimen surface after washing were the outcome of interest as they represent the firmly adherent population. Afterwards, to determine the number of adherent cells, the specimens were separately placed in new tubes filled with 1mL of sterile broth, and were shaken for 20 minutes at 150 rpm in an orbital shaking water bath. 100 µL aliquots were subsequently taken from each tube and were subjected to ten-fold serial dilutions (10^{-1}–10^{-3}). 50 µL aliquots of the dilutions and stock were subsequently streaked on agar plates using glass beads. The CFU/mL of each of these were determined after overnight incubation.

This procedure was performed 3 times on 3 different days to verify statistical validity (n=18). The total samples used for adhesion test including all the materials were (n=54) Reproducibility and reliability of data in the 3 trials were analyzed using paired samples T-tests and Pearson Correlation on SPSS Statistics software, version 25 (IBM Corp., Armonk, NY, USA).

Other trials were subsequently performed to determine the time-dependent effect of AgNPs at 3 hours and 24 hours.

2.6.2. Disk and Well Diffusion Assays

The Kirby-Bauer disk diffusion method was used to determine the diffusion assays.

Cultures were prepared using the appropriate agar plates and upside-down incubation at 37 °C overnight. Additional agar plates were prepared for the disk and well diffusion assays by autoclaving the 22.5mL agar solution prior to being poured and solidified. The microbial inoculum was prepared using sterile normal saline solution (0.9%) according to the 0.5 McFarland standard range. The sample size included 9 samples for all the materials including 1-Layer, 3 Layer and uncoated samples

A sterile cotton swab was dipped in the inoculum and streaked across the surface of agar plates thrice, rotating it 60° between each streak for even distribution. Care was taken to remove accidental splashes of extra inoculum. Uncoated and single layer-coated specimens from each material were prepared and placed on the inoculated agar plates. They were incubated overnight in an upright position.

A sterile yellow tip (10-100 µl) was used to create wells in inoculated Mueller-Hinton and Sabouraud Dextrose agars. AgNP suspension was prepared via 20-minute sonication to ensure dispersion; a portion was reserved as an ‘unfiltered’ sample, while the remainder was filtered to

 doi:10.20944/preprints202605.0288.v1

isolate the ionic fraction. Then 20 µL aliquots of filtered and unfiltered AgNP solution, deionized water (negative control), and Tigecycline (positive control) were loaded into the respective wells. The plates were incubated upright for 24 hours. The results showed no inhibition zones, which necessitated the repeated use of both 1- and 3-layers spray coated specimens for reevaluation of results with direct contact test.

2.6.3. Direct Contact Test

Uncoated, 1 layer-coated, and 3 layer-coated samples were prepared from each material (n=9) total three materials (n=27). Cultures were prepared using the appropriate agar plates and upside-down incubation at 37 °C overnight. The microbial inoculum was prepared using the appropriate broth according to the 0.5 McFarland standard range. 10 µL of the prepared mixture was placed on each specimen in their separate petri dish, covered by sterile coverslip. These were incubated for 1 hour.

Each specimen was placed separately in sterile plastic tubes, and 10 mL of sterile broth was added. These were subjected to water bath shaking for 20 minutes at 150 rpm, same as the one performed for the adhesion test. 100 µL aliquots were subsequently taken from each tube and were subjected to ten-fold serial dilutions (10^{-1}–10^{-3}). 50 µL aliquots of the dilutions and stock were subsequently streaked on agar plates using glass beads. The CFU/mL of each of these were determined after upside-down, overnight incubation.

Similar to the adhesion test, the procedure was performed over 3 trials and reproducibility and reliability of the trials were analyzed on SPSS Statistics software, version 25, using the same tests; paired samples T-tests and Pearson Correlation.

2.7. Characterization of 1-Layer Spray-Coated and Uncoated Specimens

2.7.1. Fourier Transform Infrared Spectroscopy (FTIR)

FTIR spectroscopy was utilized in (Characterization lab, Nanotechnology Institute, Jordan University of Science and Technology, Irbid, Jordan) to analyze the chemical composition and surface functionalization of the 1-layer-coated specimens.

TENSOR II FTIR Spectrometer integrated with a Platinum Attenuated Total Reflectance (ATR) accessory and a HYPERION 2000 FTIR Microscope was utilized to perform the spectral analysis. This setup allows for a wide spectral range extending from the far-infrared (FIR, 80 cm^{-1}) through the mid-infrared and even up to the visible spectrum (VIS, up to 25,000 cm^{-1}).

The Platinum ATR accessory was used for analyzing the surface of the specimens, which utilizes a high-performance single-reflection diamond crystal, helping with non-destructive analysis of solid samples and allowing for the application of high contact pressure whilst ensuring optimal optical coupling between the AgNP-coated material and the diamond crystal to provide high-sensitivity measurements across the near-infrared (NIR), mid-infrared, and far-infrared regions without need for complex sample preparation. The spectra acquired were within the range of 4000–400 cm^{-1} at a resolution of 4 cm^{-1}. The spectrum was collected by averaging 32 scans per sample.

The FTIR Microscope provided detailed microanalysis and chemical mapping, and evaluated the spatial distribution of the samples. Focal Plane Array detector was used to obtain chemical images. Data processing and the generation of 2D and 3D false-color maps were performed using OPUS software (v8.5; Bruker Optics GmbH, Ettlingen, Germany).

Standard 15× objectives were used for general sample alignment, and high-magnification (20×, 36×) objectives were used for focusing on localized NP clusters. ATR objective (20×) was utilized for transparent or reflective facial materials. High-contrast images were visualized in 2D and 3D false-color scales to represent the distribution of AgNPs surface coating.

 doi:10.20944/preprints202605.0288.v1

2.7.2. Energy Dispersive X-Ray Spectroscopy (EDS)

EDS was performed at a depth of 5 microns per area using an FESEM equipped with EDS for all 1-layer spray-coated and all uncoated samples; Acrylic (AC-blank), Silicone (Si-blank), and Zirconium (Zr-blank). The samples were coated with platinum using a sputter coater prior to imaging. Both Secondary Electron and Backscattered Electron detectors were utilized. Device details are mentioned in Table A1.

2.7.3. Energy Dispersive X-Ray Fluorescence (EDXRF)

EDXRF was additionally utilized to determine the elemental composition of the uncoated and 1-layer spray-coated specimens via Rigaku NEX QC+ spectrometer operated using QUANTEZ software (Rigaku, USA) in helium atmosphere, and a QC-14 mm diaphragm.

3. Results

The results are described in three phases, the first of which describes the results that provide the rationale behind the chosen concentration of Ag NP, and determining the optimal coating method, the number of layers, and the number of sprays per layer according to antimicrobial activity.

3.1. FESEM of Ag NP Powder

Results showed a narrow-size distribution of quasi-spherical particles with an average size of 30 nm, ranging from 18–48nm, Figure 1.

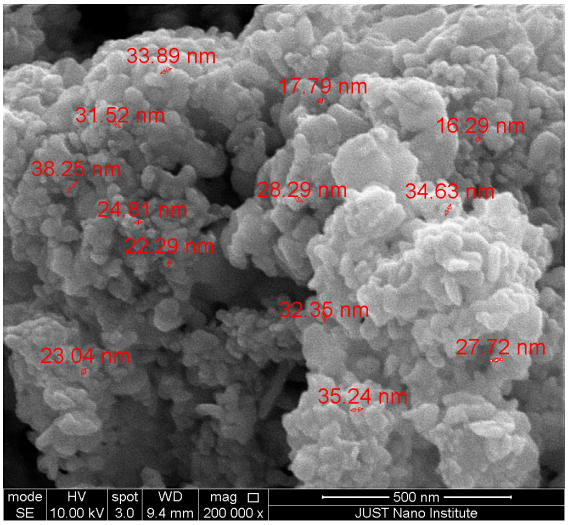

Figure 1. Powder Nanoparticles (NPs) under Field Emission Scanning Electron Microscope (FESEM).

3.2. Ag NP Concentration Selection and Suspension Characterization

3.2.1. MIC

The results are shown in Table 3. MIC was 0.0025g/mL. Wells 3 and 4 showed only partial bacterial inhibition and were therefore considered for selection since the goal was to prevent bacterial growth and subsequent biofilm formation, and preserve color aesthetics of the specimens.

 doi:10.20944/preprints202605.0288.v1

Table 3. The results of various AgNP concentrations on the growth of *P. aeruginosa.*

Well No.	AgNP Concentration (g/mL)	*P. aeruginosa*	MBC (CFU/mL after subculture, log reduction)
1	0.005	Complete Inhibition (-)	0.00*
2	0.0025	Complete Inhibition (-)	0.00*
3	0.00125	Partial Inhibition (+)	6.75×10^7, ~ 2.82
4	0.000625	Partial Inhibition (+)	6.5×10^8, ~ 1.83
5	0.0003125	Full Growth (++)	-
6-10	< 0.0003	Full Growth (++)	-
11	0 (Positive Control)	Full Growth (+++)	-
12	Broth (Negative Control)	No Growth (-)	-

* the numbers result from tenfold dilution up to 4 times. - results were not considered.

3.2.2. MBC

The results of MBC were acquired. Calculations were made based on the log reduction and percentage reduction formulas shown in Equations (2) and (3) below, respectively. The initial CFU represents positive control, and final CFU represents wells 3 and 4.

$$\log reduction = \log_{10} \frac{(initial\ CFU)}{(final\ CFU)} \quad (2)$$

$$percentage\ reduction = 100 \times \frac{initial\ CFU - final\ CFU}{initial\ CFU} \quad (3)$$

Well 3 showed a log reduction of ~ 2.82, and a percentage reduction of ~ 99.85%. Well 4 had a lower effect at log reduction ~ 1.83, and percentage reduction ~ 98.54%.

Because of the significant difference in log reduction and inhibitory effect, well 3 was favorably selected and the concentration of AgNPs chosen for the remainder of the study is 0.00125 g/mL.

3.2.3. Characterization of Ag Suspension

The Zeta potential was—26.5 mV, indicating moderate stability of the suspension, and is closely correlated with FESEM results of powder Ag NPs.

DLS showed an average hydrodynamic size of 50.54 nm (PDI: 0.5), and a primary core size of 15.19 nm; indicating a moderately polydisperse suspension, which is within the acceptable range.

3.3. Optimal Coating Method Determination

SEM was utilized for evaluation of uniformity of distribution of coating methods. Uncoated samples were first evaluated.

A comparison of the three coating techniques on acrylic shows specific variations in morphology, uniformity, and coverage, as discussed below, and shown in Figure 2.

- **Spray Coating:** exhibited better uniformity and homogeneity of deposition. The AgNPs were evenly distributed, closely following the substrate topography with low agglomeration, indicating an effective and highly controlled deposition.
- **Spin Coating:** showed a thinner and discontinuous coating. The acrylic polishing grooves remained visible, and particles appeared as scattered deposits and had localized agglomerations, indicating poor film continuity.
- **Dip Coating:** resulted in a highly heterogeneous coating, marked thickness variations, and localized agglomerations. Irregular, film-like deposits were observed with certain exposed areas, which can be attributed to gravitational effects and solvent drainage.

 doi:10.20944/preprints202605.0288.v1

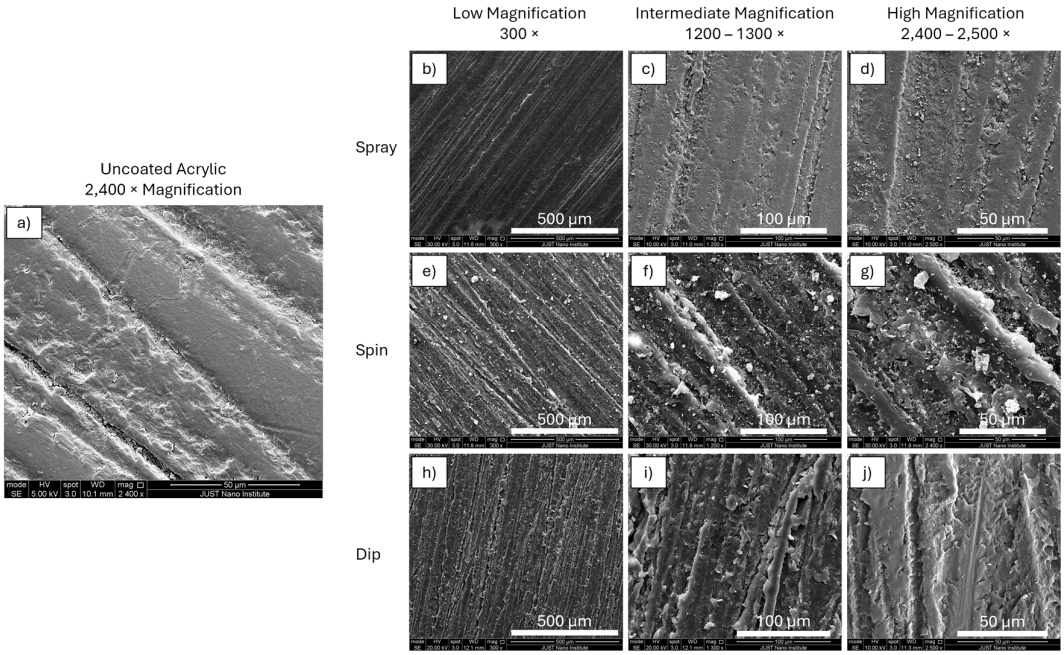

Figure 2. SEM images of (a) uncoated acrylic, and coated acrylic via (b-d) spray, (e-g) spin, (h-j) dip. Magnifications shown are 300×, 1,200× and 2,500×. Note the uniform deposition of Ag NPs in (d), compared with (g) and (j), which show agglomerations and heterogenous distribution, respectively.

Spray coating was the most effective method for achieving a homogeneous, high-coverage Ag layer on acrylic, whereas spin and dip coating resulted in inconsistent and poorly distributed films.

A comparison of the three coating techniques on silicone shows specific variations in morphology, uniformity, and coverage, as discussed below, and shown in Figure 3.

- **Spray Coating:** Revealed to be the most uniform and homogenous, where the AgNPs had equal distribution across the elastic surface texture and least agglomeration without signs of delamination, suggesting a well-controlled deposition and a powerful adhesion.
- **Spin Coating:** Exhibited thin, incomplete and discontinuous coating where the surface remained partially exposed between discrete, isolated particles and tiny clusters, suggesting discontinuous film and localized agglomerates.
- **Dip Coating:** Showed noticeably high heterogeneity and pronounced thickness variations, with large areas of bare surfaces and irregular micro-agglomerations, indicating low-uniformity and unequal deposition.

As a result, spray coating was the most effective technique for a more homogenous, uniform, and complete Ag NP film formation on silicone.

A comparison of the three coating techniques on Zirconium shows specific variations in morphology, uniformity, and coverage, as discussed below, and shown in Figure 4.

- **Spray Coating:** Showed a continuous, uniform coating where the AgNPs appeared as evenly distributed discrete particles and tine clusters over a broad area, without significant delamination or cracking, suggesting a strong and effective adhesion.
- **Spin Coating:** Revealed thin, discontinuous, and incomplete film formation, with few surface AgNP deposits, preferential accumulation along polishing grooves, and prominent underlying surface features.
- **Dip Coating:** Exhibited a heterogenous, non-uniform film formation and markedly varying thickness, characterized by uneven and irregular AgNP distribution and large uncoated areas which can be attributed to gravitational effects and solvent drainage in the withdrawal process.

 doi:10.20944/preprints202605.0288.v1

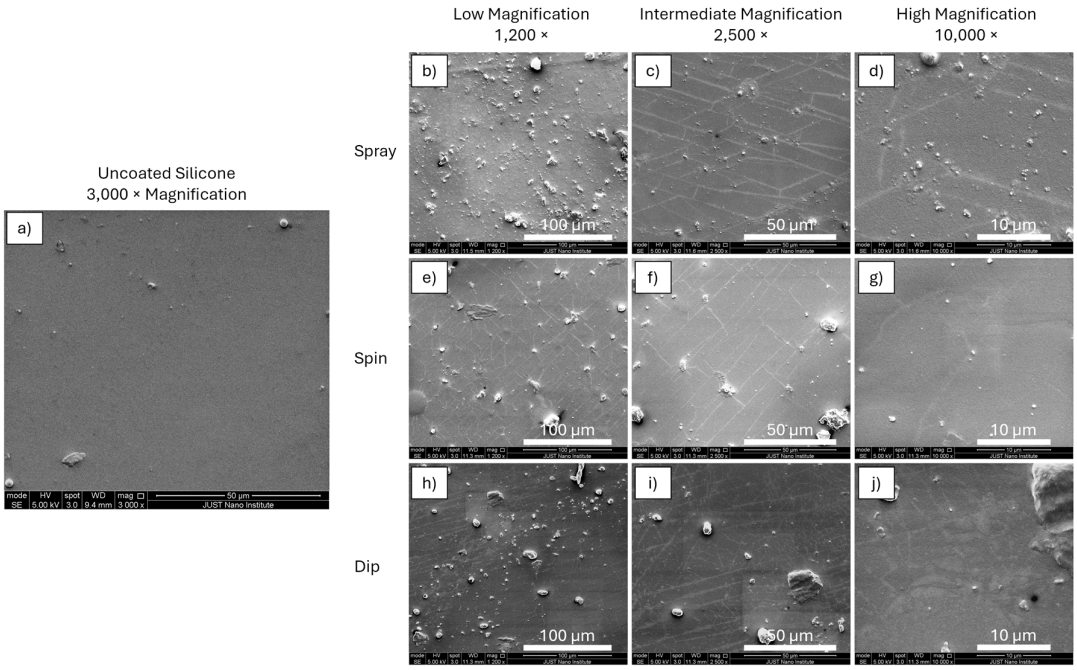

Figure 3. SEM images of (a) uncoated silicone, and coated silicone via (b-d) spray, (e-g) spin, (h-j) dip. Magnifications shown are 1,200×, 2,500×, and 10,000 ×.

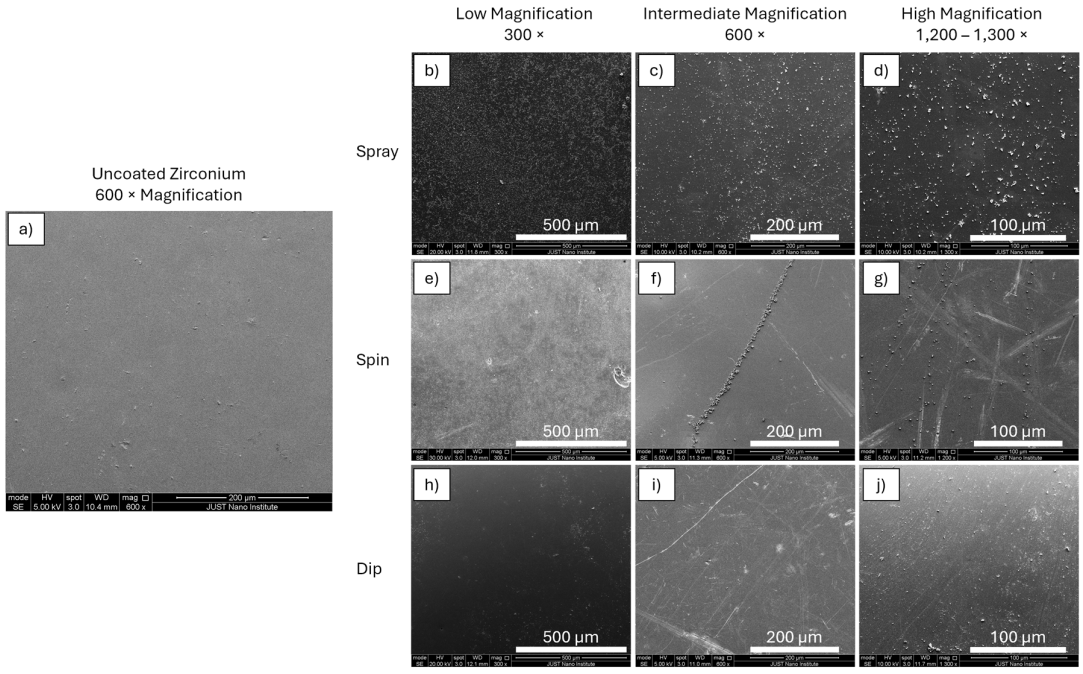

Figure 4. SEM images of (a) uncoated zirconium, and coated zirconium via (b-d) spray, (e-g) spin, (h-j) dip. Magnifications shown are 300×, 600×, and 1,200-1,300×.

Spray coating exhibits the highest coverage and most stable Ag layer formation, and is the most effective method among the mentioned coating techniques for zirconium.

Due to the overall favorable SEM results of spray coating, as shown in Table 4, this coating method was used for the remainder of the study.

 doi:10.20944/preprints202605.0288.v1

Table 4. Overall SEM results of coating methods for all materials.

Method	Morphology (generalized)	Uniformity	Coverage	Consistency across materials
Spray	Continuous / substrate-following	High	Complete	Consistent
Spin	Discontinuous / clustered / thin	Low	Incomplete	Consistent
Dip	Heterogeneous / irregular / thicker	Low	Incomplete	Consistent

3.4. Selection of Optimum Number of Layers for Spray Coating

3.4.1. Adhesion Test

The reliability results show a strong positive correlation between all 3 trials (Table 5), and Pearson correlation coefficients ranges from 0.717–0.941 ($p < 0.05$). In addition, the paired samples test (Table 6) shows no significant differences between the mean bacterial contents of the trials ($p > 0.05$), confirming the high reproducibility and stability of the coating and testing methodology.

Table 5. Results finding correlation reliability of adhesion tests between the three trials using paired samples correlations. The bacterial content of all materials and both layers have been taken into consideration.

Trials	N	Correlation	Sig.
Comparison between Trial 1 and Trial 2	9	0.717	0.030
Comparison between Trial 1 and Trial 3	9	0.898	0.001
Comparison between Trial 2 and Trial 3	9	0.941	0.000

Table 6. Results presenting differences of results in pairs spray-coated AgNP for the three adhesion trials using paired samples test. The bacterial content of all materials and both layers have been taken into consideration.

	Paired Differences			t	df	Sig. (2-tailed)
	Mean	Std. Deviation	Std. Error Mean			
Comparison between Trial 1 and Trial 2	-470022	725730	241910	-1.943	8	0.088
Comparison between Trial 1 and Trial 3	-490777	857039	285679	-1.718	8	0.124
Comparison between Trial 2 and Trial 3	-20755	341132	113710	-0.183	8	0.860

The results showed significantly lower microbes in coated than uncoated specimens. Additionally, one-layer coating was determined as the optimal number for *P. aeruginosa*, additional details are shown in Table 7.

Table 7. Results for antimicrobial activity of adhesion test of 1- and 3-layer spray-coated AgNP for Acrylic, Silicone, and Zirconium against *P. aeruginosa.*

Material	*P. aeruginosa*
Acrylic	3-layer coat is better
Silicone	1-layer coat is better
Zirconium	No significant difference

The 1-layer was preferably chosen over the 3-layers since it made no significant difference in adhesion test, and to reduce the risk of potential surface aggregations and color instability.

 doi:10.20944/preprints202605.0288.v1

3.4.2. Disk and Well Diffusion Assays

The results showed no inhibition zones, which necessitated the repeated use of both 1- and 3-layers spray coated specimens for reevaluation of results with direct contact test.

3.4.3. Direct Contact Test

A significant correlation was observed between trials 1 and 2 ($r = 0.887$, $p = 0.001$) and trials 2 and 3 ($r = 0.809$, $p = 0.008$). And, although the correlation between Trial 1 and 3 was moderate and non-significant ($r = 0.541$, $p > 0.05$), the paired samples t-test confirmed there were no statistically significant differences between the mean results of any trial pair ($p > 0.05$), indicating reproducibility, and suitability for comparative analysis despite the intrinsic biological variations in direct contact tests. As shown in Tables 8 and 9.

Table 8. Results finding correlation reliability of direct contact tests between the three trials using paired samples correlations. The bacterial content of all materials and both layers have been taken into consideration.

	N	Correlation	Sig.
Comparison between Trial 1 and Trial 2	9	0.887	0.001
Comparison between Trial 1 and Trial 3	9	0.541	0.132
Comparison between Trial 2 and Trial 3	9	0.809	0.008

Table 9. Results presenting differences of results in pairs spray-coated AgNP for the three direct contact trials using paired samples test.

	Paired Differences			t	df	Sig. (2-tailed)
	Mean	Std. Deviation	Std. Error Mean			
Comparison between Trial 1 and Trial 2	-4255.6	7808.1	2602.7	-1.635	8	0.141
Comparison between Trial 1 and Trial 3	4571.1	10371.4	3457.1	1.322	8	0.223
Comparison between Trial 2 and Trial 3	8826.7	14648.3	4882.8	1.808	8	0.108

The results showed significantly lower microbes in coated than uncoated specimens. However, unlike in the adhesion test, the direct contact test results show that the optimal number of layers depend varyingly on the material and microbe, as depicted in Table 10.

Table 10. Results for antimicrobial activity of adhesion test of 1- and 3-layer spray-coated AgNP for Acrylic, Silicone, and Zirconium against P. aeruginosa.

Material	***P. aeruginosa***
Acrylic	1-layer coat is better
Silicone	1-layer coat is better
Zirconium	3-layer coat is slightly better

3.5. Characterization of 1-Layer Spray-Coated and Uncoated Specimens

3.5.1. FTIR

FTIR of the samples were obtained from five different regions of the same specimen, however the curves of only two regions are depicted in Figures 5–7. FTIR spectra of uncoated acrylic samples exhibits absorption bands characteristic of acrylic/PMMA, as shown in Figure 5 and revealed additional strong ester carbonyl bands at ~1726 cm^{-1}, C–H stretching around ~2943 cm^{-1}, and deformation bands near ~1443 and ~1391 cm^{-1}. The fingerprint region showed prominent ester/C–O–C related bands at ~1248 and ~1145 cm^{-1}, and additional PMMA fingerprint peaks around ~980, ~836, ~752 and ~663 cm^{-1} were observed. No additional peaks or band shifts were obtained across the measured areas, indicating no newly-formed functional groups. The peak positions were

 doi:10.20944/preprints202605.0288.v1

reproducible in all the five measured regions, suggesting chemical uniformity across uncoated acrylic surface.

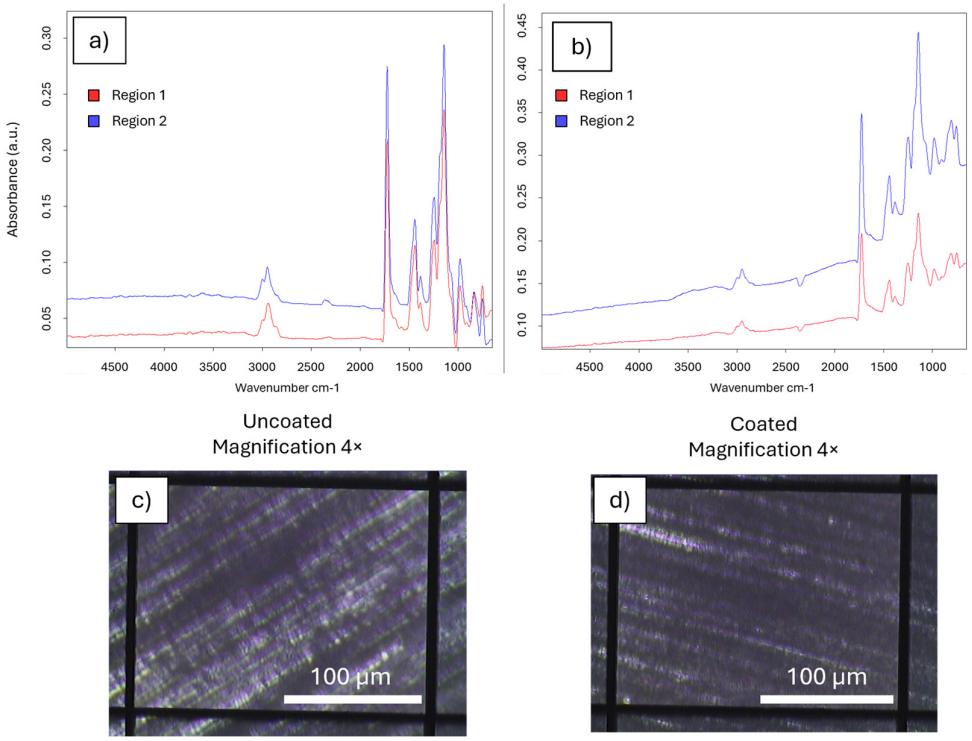

Figure 5. FTIR spectra of; a) uncoated, and b) coated acrylic. Note that FTIR of PMMA material confirm the chemical structure without the presence of new peaks indicating that no altering the chemical composition of the material has been observed and the silver nanoparticle has been deposited on the surface successfully. FTIR images of c) uncoated and d) coated acrylic.

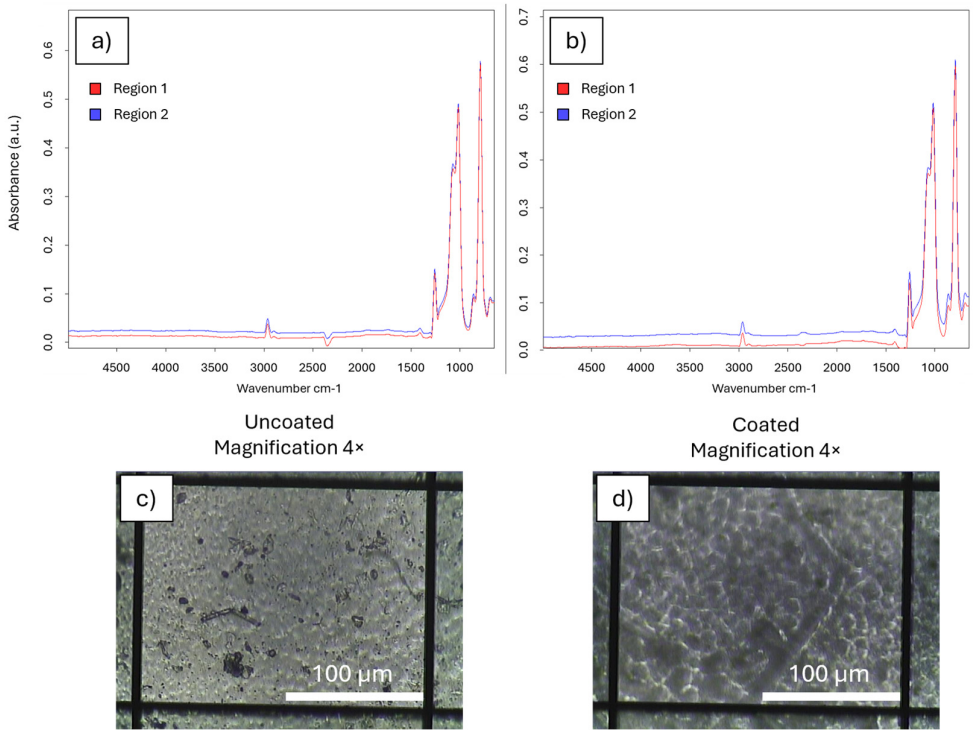

 doi:10.20944/preprints202605.0288.v1

Figure 6. FTIR spectra and images of; a) and c) uncoated, and b) and d) coated silicone.The FTIR spectra shows the chemical adsorption of the sillicone material with no additional peaks or shifing confirming the successful deposition of the silver nanoparticle without altering the chemical compostion of the material.

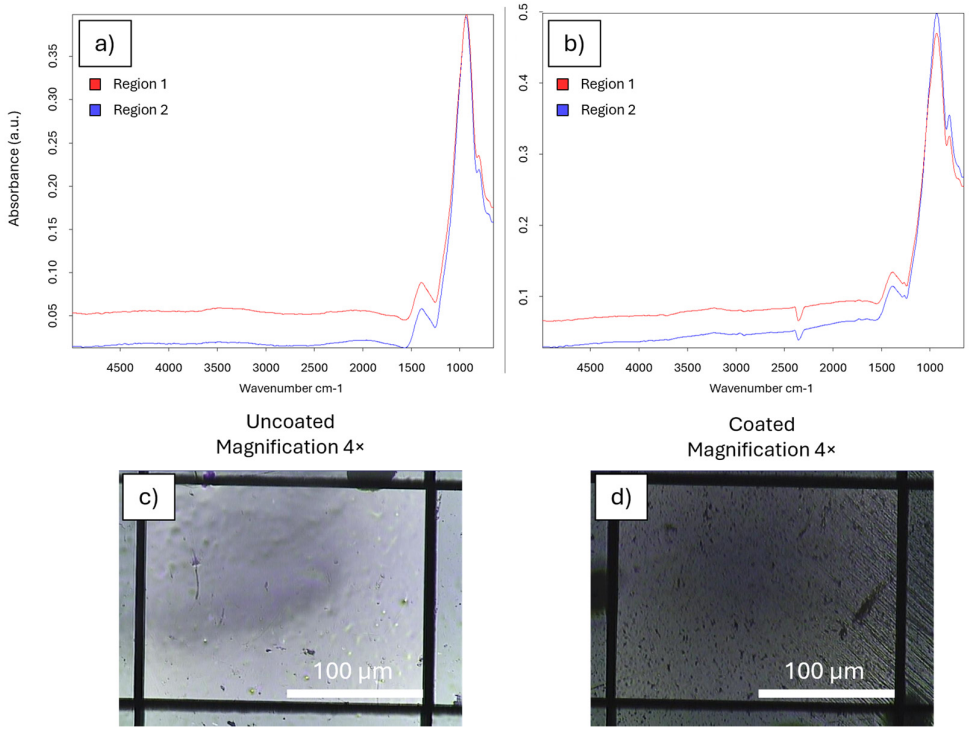

Figure 7. FTIR spectra and images of; a) and c) uncoated, and b) and d) coated zirconium. The FTIR shows the charactaristic of zirconium material with are Zr_O and Zr_O_Zr, the coatead samples didn't show new functional groups or peaks confirming the physical deposition of the silver nanoparticle on the surface of the material without chemical alteration of specimen material.

FTIR spectra of Ag-coated acrylic samples showed absorption bands characteristic of PMMA; C–H stretching at ~2940 cm^{-1} and a strong ester C=O stretching band at ~1725 cm^{-1}. Additional bands corresponding to CH_3 bending (~1440 and ~1390 cm^{-1}) and C–O/C–O–C stretching (~1245 and ~1140 cm^{-1}) were also seen. The Ag-coated acrylic, when compared with uncoated acrylic, reveal a notable reduction in peak intensities and some band broadening which can result from the Ag coating, as shown in Figure 5. No new absorption bands that indicate chemical changes or new functional group formation of PMMA matrix were observed. These confirm surface coating without chemical modifications.

Figure 6 showcases the FTIR results of both uncoated and coated silicone. The uncoated silicone samples showed C–H stretching in the range of 2960–2900 cm^{-1}. The strong absorption band in the range of 1090–1020 cm^{-1} was attributed to asymmetric stretching of the Si–O–Si backbone, which confirms the silicone polymer structure. Bands in the range of 800–860 cm^{-1} represents Si–C stretching, and bands at ~1260 cm^{-1} represent Si–CH_3 deformation. These exhibit characteristic absorption bands of polydimethylsiloxane. No additional peaks or shifts indicate lack of chemical alterations, confirming absence of prior sample modification.

The Ag-coated silicone samples reveal absorption bands characteristic of PDMS; C–H stretching between 2960–2900 cm^{-1}, strong asymmetric Si–O–Si stretching in the range of 1090–1020 cm^{-1}, Si–CH_3 stretching at ~1260 cm^{-1} indicating deformation, and Si–C stretching at ~800–860 cm^{-1} were detected. There were no newly observed absorption bands.

 doi:10.20944/preprints202605.0288.v1

Similar to acrylic, the Ag-coated silicone revealed minimal peak broadening and decreased band intensities compared with the uncoated sample, as shown in Figure 6. This can be associated with the Ag NP coating. The absence of new absorption bands suggest that the coating process did not chemically modify the silicone polymer, and the AgNPs were physically deposited rather than form chemical bonds represented by lack of new functional groups.

The uncoated and coated zirconium FTIR results are shown in Figure 7. The uncoated zirconium specimens showed prominent bands at ~935–940 cm^{-1} and 800–810 cm^{-1}, which represent Zr–O and Zr–O–Zr lattice vibrations, respectively. These are characteristic of zirconia. Slight peaks at ~2350–2365 cm^{-1} may be related to atmospheric CO_2, and weak bands ~1380–1400 cm^{-1} can be attributed to surface carbonate species. The results from different regions were highly similar, suggesting high chemical uniformity of the samples.

The Ag-coated zirconium samples revealed typical absorption bands of zirconia: the eminent peaks at ~935–940 cm^{-1} and 800–810 cm^{-1} representing Zr–O and Zr–O–Zr lattice vibrations, respectively. And the small bands ~2350–2365 cm^{-1} and ~1380–1400 cm^{-1} that could be attributed to atmospheric CO_2 and surface carbonate, respectively. See Figure 6.

The reduced intensities and peak broadening, and the absence of new absorption bands and new functional groups, indicate a physically deposited coverage with Ag NPs without chemical alterations of the zirconium.

3.5.2. EDS

Uncoated (AC-blank) and coated (AC-spray) acrylic specimen results are depicted in Figure 8.

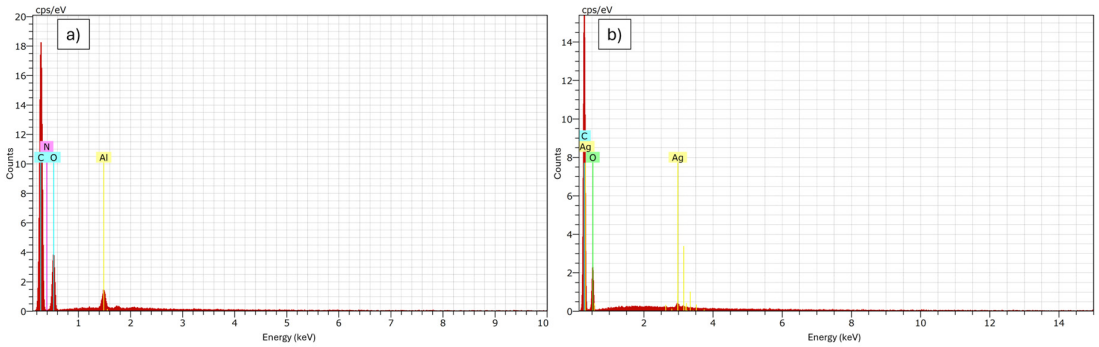

Figure 8. EDS spectra graphs of a) uncoated, and b) coated acrylic. Note that the C and O are the main elements and in the coated samples clearly confirms the presence of the Ag, however after coating leading to a slight change of the C and O amount due to the surface depostion of Ag nanoparticle.

The EDS results of the AC-blank shows C as the primary element, and O as the second most common, a result consistent with the chemical composition of PMMA which comprises mainly of C– and O– containing functional groups. The C peak corresponds to the polymer backbone of acrylic resin, and the O peak represents the ester functional groups –COO–. A minimal aluminum (Al) peak was found, indicating a trace amount of the material, which is unlikely from the acrylic material and can be attributed to sample holder contamination, polishing residues, or environmental background. The specimen result can be used as a valid control group since no Ag or other coating-related elements were present, confirming the chemical purity of the sample and the uncoated surface.

In AC-spray, Ag peaks were detected, especially the Ag L-series, which suggests the presence of Ag on the coated acrylic and a successful Ag NP deposition. C and O were also detected; the primary elements of acrylic substrate. A further support for the formation of a uniform coating is the aforementioned homogenous distribution of the spray-coated Ag viewed on the SEM.

The EDS results of Si-blank, shown in Figure 9a, reveals Si as the primary element, and a strong O peak, consistent with the composition of Si-based materials and corresponding to the materials'

 doi:10.20944/preprints202605.0288.v1

siloxane backbone Si–O–Si. The C peaks either have very low intensity or are absent. This result is expected in Si-based, primarily inorganic materials. The sample is suitable as a control group due to absence of Ag or other coating-related elements.

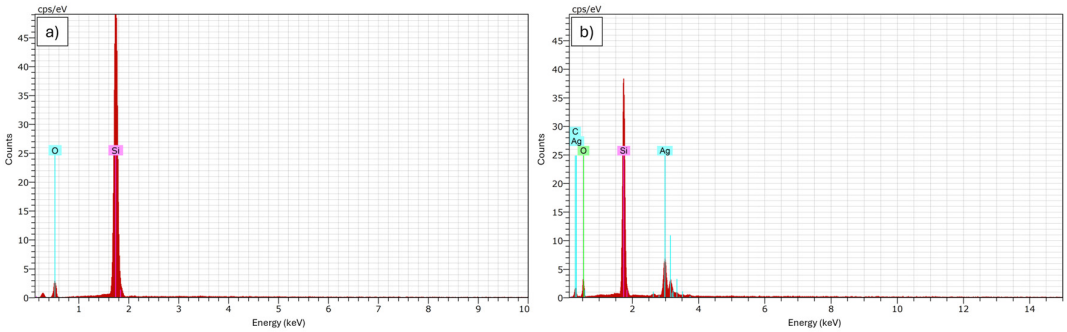

Figure 9. EDS spectra graphs of a) uncoated, and b) coated silicone. The EDS analysis shows Si and O are the primary elements of the maxillofacial silicone, the presence of the silver peaks in coated specimens confirms the successful presence of the silver nanoparticle, the decrease in the Si element may be due to the presence of the Ag nanoparticle.

Clear Ag peaks were observed in Si-spray (Figure 9b), indicating the presence and successful deposition of Ag NPs onto the surface. The characteristic elements of the silicone substrate were still present; Si and O. And minimal amounts of C were additionally observed and could be attributed to the organic silicone matrix or to surface contamination.

Zr-blank EDS spectra also revealed peaks consistent with the main elements; ZrO_2, with Zr being the predominant element, followed by O, as shown in Figure 10a. The high Zr peak not only verifies the ceramic nature of the material, but also shows the integrity of the surface. The O peak represents the oxide phase of zirconia, indicating a stable Zr–O bonding. Low C peaks can be caused by carbon tape (used during sample mounting), surface contamination, or atmospheric carbon deposition. The trace levels of Al can be due to polishing residues or environmental contamination. The sample can be used as a control group due to lack of Ag or other coating-related elements.

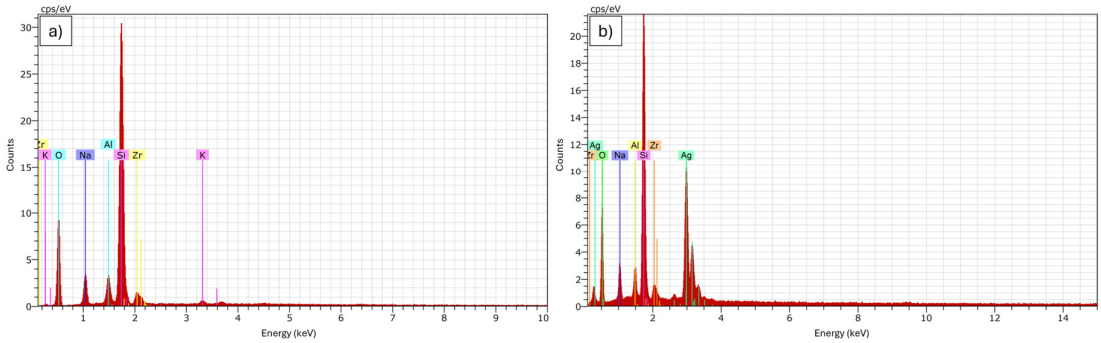

Figure 10. EDS spectra graphs of a) uncoated, and b) coated zirconium. The EDS spectra shows that the Zr and the O are the primary elements of the specimen.Note that the absence of the Ag in the uncoated samples while the presence of the Ag in the coated samples confirming the presence of silver nanoparticle of the spray coated specimen.

Figure 10b displays the spectra of Zr-spray, which detected the innate elements of Zr and O in the substrate, and additionally detected Ag peaks, indicating successful Ag NP deposition onto the substrate surface.

 doi:10.20944/preprints202605.0288.v1

3.5.3. EDXRF

In the uncoated acrylic specimen (AC-Blank), Ag was not detected, confirming the absence of silver in the substrate material prior to coating. The elemental composition of AC-Blank was dominated by Fe (52.1 mass%), Ba (18.5 mass%), and Ti (11.1 mass%), with additional minor constituents including S (2.39 mass%), Ni (3.47 mass%), V (3.30 mass%), and Sr (1.08 mass%).

In the 1-layer AgNP-coated acrylic (AC-1L), Ag was detected and quantified at 0.205 mass% (statistical error ±0.012 mass%), well above both the LLD (0.0262 mass%) and LLQ (0.0787 mass%). The silver signal was identified via the Ag-Kα emission line (intensity: 0.48425 cps/μA). The overall elemental profile of the coated specimen differed substantially from the blank, with Al (56.8 mass%) and Si (8.81 mass%) dominating the spectrum, potentially reflecting the inorganic filler composition exposed at the specimen surface, alongside Fe (9.35 mass%), S (3.30 mass%), Cl (2.93 mass%), Ba (1.72 mass%), and Ni (3.48 mass%). The presence of chlorine (2.93 mass%) in the coated specimen, absent from the blank, is consistent with residual Cl from the AgNP aqueous suspension.

The detection of silver at 0.205 mass% in the coated specimen and its complete absence in the uncoated control provides quantitative XRF confirmation that the spray-coating procedure successfully delivered AgNPs onto the acrylic surface in a single application cycle, without requiring chemical modification of the substrate or the addition of binder or coupling agents.

In the uncoated silicone (Si-Blank), the spectrum was dominated by Si at 98.8 mass%, consistent with the silicone matrix, and minor constituents including Al (0.385 mass%), S (0.101 mass%), Ti (0.180 mass%), V (0.0725 mass%), Fe (0.189 mass%), Ni (0.0863 mass%), and Ba (0.144 mass%). Ag was detected only at a trace level of 0.0014 mass% (statistical error ±0.0002 mass%), which is essentially at the instrument's quantification threshold for Ag (LLQ 0.0013 mass%, LLD 0.0004 mass%). This indicates that the uncoated silicone contains no meaningful Ag signal beyond trace-level detection.

After 1-layer coating (Si-1L), Ag was clearly detected and quantified at 0.0071 mass% (±0.0002 mass%), which is well above both the Ag LLD (0.0004 mass%) and LLQ (0.0013 mass%). The Ag signal was identified via the Ag-Kα emission line (intensity 1.26257 cps/μA). The coated specimen retained a silicone-dominant composition (Si 98.5 mass%) with similar minor constituents to the blank, while Cl increased from 0.0380 mass% (blank) to 0.0729 mass% (coated), consistent with residual chloride associated with the deposited AgNP suspension. Overall, the XRF results confirm successful deposition of Ag onto the silicone surface after a single spray-coating cycle.

The uncoated zirconia (Zr-Blank), the spectrum was dominated by Si (41.7 mass%) and Zr (36.3 mass%; Zr-Kα intensity 5467.3 cps/μA), and additional constituents included Na (10.5 mass%), Al (3.96 mass%), yttrium (2.31 mass%, consistent with yttria-stabilized dental zirconia), hafnium (0.900 mass%), K (1.48 mass%), Ni (0.646 mass%), Ca (0.733 mass%), Ti (0.464 mass%), and erbium (0.294 mass%). Ag was not detected in the blank (ND; Ag LLD 0.0018 mass%, LLQ 0.0055 mass%)

In 1-layer coated zirconium (Zr-1L), Ag was detected and quantified at 0.0206 mass% (±0.0013 mass%; Ag-Kα intensity 0.8075 cps/μA), well above both the LLD and LLQ, confirming successful deposition of Ag onto the surface. The Ag peaks (Ag-Kα and Ag-Kβ1) were present in the coated specimen's high-Z spectral region and absent in the blank. Importantly, the dominant substrate elements remained similar after coating (Zr 37.4 mass%, Si 39.9 mass%, Na 11.0 mass%, Al 4.06 mass%, Y 2.36 mass%, Hf 0.914 mass%, Er 0.238 mass%), indicating that the coating procedure did not alter the zirconia's bulk elemental composition and that the detected Ag represents a surface deposit. Chlorine was below the detection limit in both zirconia specimens, suggesting no measurable chloride accumulation on this substrate under the coating conditions used. Overall, XRF gives quantitative confirmation that a 1 layer spray-coating produced a measurable silver-containing surface layer on glazed zirconia without causing substantial elemental contamination.

3.6. Details of Antimicrobial Performance

3.6.1. Adhesion Test

 doi:10.20944/preprints202605.0288.v1

The comparative analysis of bacterial adhesion across the three substrate materials showed a significant correlation between the 1-hour adhesion results of all 3 materials ($p < 0.05$), and the strongest correlation observed is between Silicone and Zirconium ($r = 0.805$, $p = 0.009$), indicating a consistent trend in microbial adhesion across the surfaces of different materials, observed in Table 11.

Table 11. Results finding correlation of adhesion tests between Acrylic, Silicone, and Zirconium using paired samples correlations. Bacterial content of both layers and average of all three trials for each material have been taken into consideration.

Material pairs	N	Correlation	Sig.
Comparison between Acrylic and Silicone	9	0.717	0.030
Comparison between Acrylic and Zirconium	9	0.765	0.016
Comparison between Silicone and Zirconium	9	0.805	0.009

However, the Paired Samples Test (Table 12), revealed that acrylic performed significantly differently from both Silicone ($p = 0.026$) and Zirconium ($p = 0.017$), as indicated by the large positive mean differences of 904,622 and 876,577, respectively. On the other hand, the comparison between Silicone and Zirconium showed no significant difference ($p = 0.668$), suggesting that these two materials provide a statistically close level of resistance to bacterial adhesion.

Table 12. Results presenting differences spray-coated AgNP for Acrylic, Silicone, and Zirconium using paired samples test. Bacterial content of both layers and average of all three trials for each material have been taken into consideration.

Material pairs	Paired Differences			t	df	Sig. (2-tailed)
	Mean	Std. Deviation	Std. Error Mean			
Comparison between Acrylic and Silicone	904622	991470	330490	2.737	8	0.026
Comparison between Acrylic and Zirconium	876577	874241	291414	3.008	8	0.017
Comparison between Silicone and Zirconium	-28044	189188	63063	-0.445	8	0.668

3.6.2. Direct Contact Test

The comparative performance of the three materials using Pearson correlation analysis revealed highly significant relationships between all material pairs ($r > 0.85$, $p < 0.005$), indicating a highly uniform response to the coating treatments across different substrates.

Notably, the paired samples t-test showed no statistically significant differences in bacterial content between Acrylic, Silicone, and Zirconium ($p > 0.05$ for all pairs). This suggests that while these materials performed differently in the Adhesion assays, they exhibit comparable antimicrobial efficacy when evaluated via the Direct Contact method.

3.7. Details of Results and Trends of Tests

3.7.1. Antimicrobial Performance for 1-Hour Adhesion and Direct Contact Tests

For obtaining simpler and clearer results the content of bacteria per each case or sample has been determined regarding control sample to be 100%, showed numbers are all in percentage to the control reference, as clearly illustrated in Figures 11–13.

Figure 11 shows that direct contact in general showed less percentage of bacteria present in comparison to adhesion tests for the 3 materials and for both types of layering, in addition to less fluctuations in percentages of bacteria content.

 doi:10.20944/preprints202605.0288.v1

Regarding each material, Zirconium shows less magnitude and less fluctuation in both tests, indicating better antimicrobial performance. Highest content of bacteria is found with Silicone material, then Acrylic. Regarding the number of layers, the bacterial content in 1-layer was less than 3-layer coating, except for zirconium, in general.

The adhesion test shows differences between both materials and layers; Silicone favors 1-Layer while Acrylic favors 3-Layer, Zirconium showed no clear preferences for the number of layers in adhesion test.

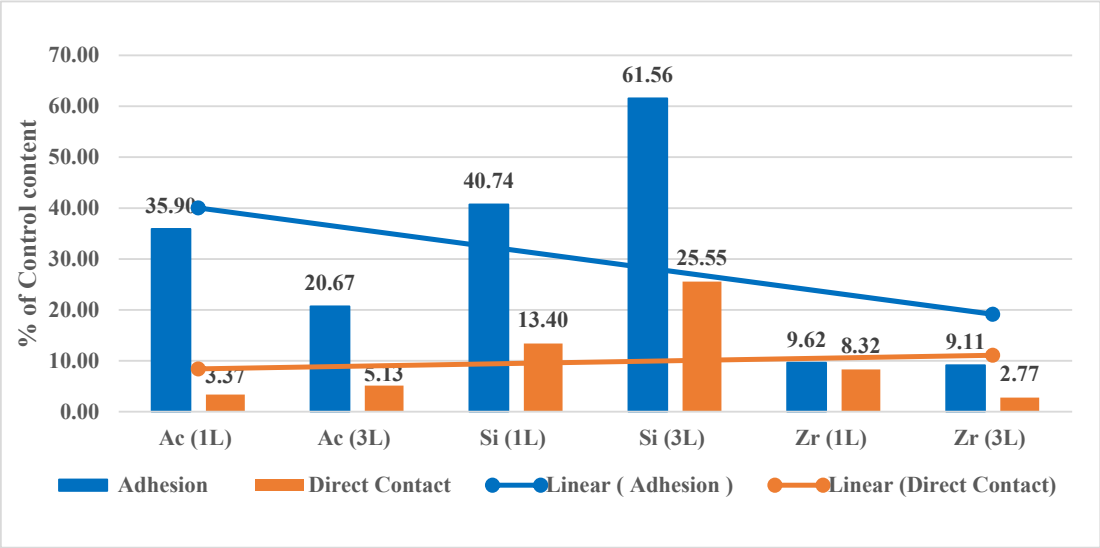

Figure 11. Percentage of bacteria remianing on different material surfaces coated with 1- and 3- layer Ag NP after adhesion and direct contact tests.

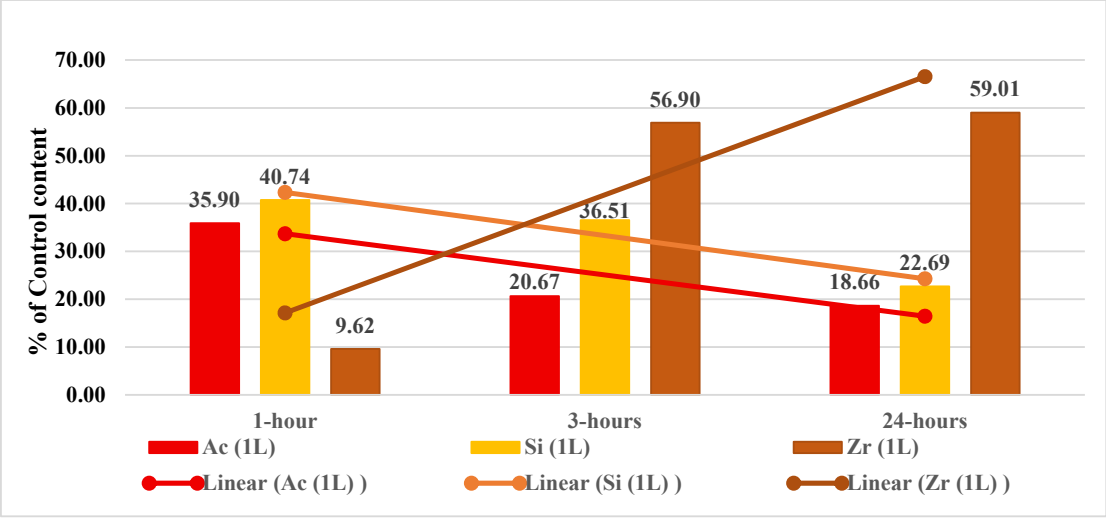

Figure 12. Bacteria content for the Acrylic, Silicone, and Zirconium materials during stages of 1-, 3-, and 24-hour stages specific with 1-Layer coating.

 doi:10.20944/preprints202605.0288.v1

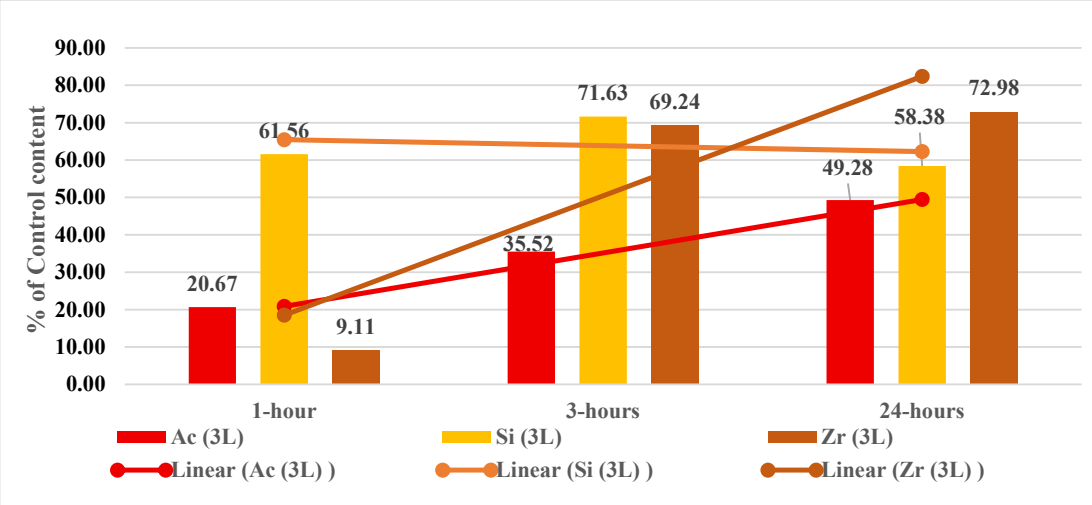

Figure 13. Bacteria content for the Acrylic, Silicone, and Zirconium materials during stages of 1-, 3-, and 24-hour stages specifically with 3-Layers coating.

3.7.2. Antimicrobial Performance and Trends for 1-, 3-, and 24-Hour(s) Adhesion Test

Observing time effect fluctuations for Adhesion tests performed for three stages 1-hr, 3-hrs and 24-hrs are presented in figures 12 and 13. Figure 12 emphasizes changes for the three materials using 1-Layer coating. Here both Acrylic and Silicone showed a clearly negative time-trend from 1-hour towards 24-hours, with Zirconium increasing trend from the 1st to 3rd hour, then plateauing at 24th hour.

For 3-Layer tests throughout the 24 hours, shown in Figure 13, the results showed a generally higher presence of bacteria than those of 1-Layer tests for the same times. Acrylic and Zirconium showed increasing bacterial content across the 24 hours, Silicone showed an overall slight decrease across the 24 hours. Average trend of the three materials with the 3-Layer coating showed clearly lower antimicrobial performance than the 1-Layer tests along 24 hours. These findings support the 1-layer coating in Adhesion tests as clearly more reliable for use in succeeding tests and applications. And although 3-layer coated Silicone in 3rd hour of the test showed a slightly increased bacterial content, the overall trend for Silicone in both layers remains the same; decreasing bacteria content overtime. All three materials, particularly Zirconium, showed clearly worse antimicrobial performance for 3-layers coating when compared with 1-layer coating in Adhesion test across 24 hours. Table 13 shows the general results for the different layer coatings across the three materials in both adhesion and direct contact tests.

Table 13. Layer coating preference for all three materials in adhesion and direct contact tests throughout the study.

	Adhesion tests	Direct contact tests
Acrylic	1-layer coat is better	1-layer coat is better
Silicone	1-layer coat is better	1-layer coat is better
Zirconium	1-layer coat is better	3-layer coat is slightly better

4. Discussion

This study investigated three Ag NP coating methods (spray, dip, spin) on three medically important facial materials (acrylic, silicone, zirconium) to determine the impact of antimicrobial properties on *P. aeruginosa*; a gram negative bacillus associated with opportunistic infections in those with decreased immune functions. [24]

 doi:10.20944/preprints202605.0288.v1

The coating methods provide thin-film coating, are inexpensive and have high-quality and thus were selected for the study [25]. The materials were chosen based on their frequent use and/or their susceptibility to infection. *P. aeruginosa* was considered since the population that is predisposed to infections by it (i.e., immunocompromised individuals), has a correlation with the population that tends to have medical need of the mentioned facial materials.

P. aeruginosa is not a part of the normal flora in the oral cavity, and in those individuals who have intact mucosal defenses, the primary flora is predominated by commensal streptococci, *Prevotella*, *Fusobacterium*, and *Veillonella* species. *P. aeruginosa* is not primarily associated with this early colonizing community [26]. Thus, detecting it usually indicates a disrupted host defense, and their numbers rise significantly with advancing age, systemic illness, hospitalization, and compromised oral hygiene [27,28]. This is clearly seen in studies detecting the rate of *P. aeruginosa* in the oral cavity of elderly patients who receive tube feeding, where the rate increases to 34% and 53%, as opposed to the orally fed patients who had lower rates between 3.3–7.5% [29,30].

However, if *P. aeruginosa* establishes in the oral cavity, it occurs primarily on removable dental prostheses, and has been observed to be the most abundant respiratory pathogen on denture surfaces and is regularly recovered from prosthetic surfaces [31,32]. *P. aeruginosa* is particularly known to begin a rapid transcriptional response specific to the surface within the 1st hour of contact and can activate adhesion-related and metabolic genes, accelerating surface adhesion [33].

This creates a reservoir from which in a reduced host defense can result in healthcare-associated pneumonia, bacteremia, and septicemia [31]. The treatment of established infections is complicated by its extreme antibiotic resistance profile. A study by Silva, et al. [34] revealed that 37.5% of isolates from ICU patients with oral colonization were multidrug-resistant, and had non-susceptibility to carbapenems and fluoroquinolones at rates of 43% and 47%, respectively. *P. aeruginosa* resistance to antibiotics is markedly higher in the biofilm state, around 100- to 1,000-fold higher than the planktonic form [35]. Thus, by targeting their initial reversible adhesion biofilm formation can be prevented [13]. This provides an additional rationale for the adhesion testing of the study; the prevention of adhesion can reduce or prevent biofilm formation. However, a more comprehensive biofilm evaluation is necessary for confirmation.

The broad-spectrum antimicrobial properties of Ag and Ag NPs, especially against both gram-negative and positive bacteria, the ability to be effective even at low concentrations, and the lack of development of resistant microbial strains, made them a favorable choice for coating [36,37].

The antimicrobial mechanism of action of Ag NPs is different from those of previous agents, and is frequently attributed to Ag ion release causing oxidative stress and DNA damage, protein dysfunction, and bacterial membrane damage [38,39]. More recent studies however reveal that the NPs themselves, through direct membrane contact, have antibacterial properties [37]. This is in direct agreement with the findings of the results section, where direct contact test exhibited higher bactericidal activity.

MBC of *P. aeruginosa* of the current study (0.00125g/mL) is five times higher than the MIC findings utilized by Alhosani, et al. [40], where the concentration needed for biofilm inhibition using ZnOAg was 0.00025g/mL. This difference in antimicrobial activity concentration may be caused by the different strains of *P. aeruginosa* used, different NP synthesis, the smaller NP size, and/or the synergistic activity of ZnO with Ag.

It can also be explained by the fact that our study utilized commercially available NPs, which usually requires higher concentrations for similar antimicrobial activity (>0.004096g/mL) compared with other methods of AgNP synthesis, and that in vitro studies require higher NP concentrations due to lack of antimicrobial properties of saliva[41].

In this context, according to Shayo, Elimbinzi and Shao [12] U.S. Environmental Protection Agency (EPA) has limited the maximal admissible AgNP exposure to 0.1mg/L. However, an official safety limit for exposure has not yet been determined and regulatory gaps still persist [42].

 doi:10.20944/preprints202605.0288.v1

Although our concentration used value in comparison is higher (1,250mg/L), this concentration is lower than the concentration required for antimicrobial activity of commercial Ag NPs (>0.004096g/mL), as mentioned by Tabassum, Khan, Jeong, Jo and Kim [41].

However, because this concentration is not fully representative of the exact amount of Ag NPs on the coated samples, XRF results were utilized to determine the more accurate amount.

Thus, following the data acquired from XRF, the amount of Ag NP per area of each material is depicted in (Table 14). This amount was determined by calculating the mass of each material disk by multiplying the volume with the density of each material [43–45]. Then, the amount of Ag per disk was calculated by the percentage provided in XRF results. Later, the amount per disk was divided by surface area per cm^2 to compare with the available cytotoxicity data in the literature.

Table 14. Ag concentration per area of different materials.

Material	Ag NPs per coated surface area
Acrylic	~488 μg/cm^2
Silicone	~12.5–14.8 μg/cm^2
Zirconium	~247–258 μg/cm^2

Agarwal, et al. [46] examined the cytotoxicity of AgNPs, where at a concentration of 0.4 μg/cm^2, the polyelectrolyte films were antibacterial and not cytotoxic, whilst they were cytotoxic to mouse fibroblasts at a concentration of ~100 μg/cm^2. Another study following (ISO10993-5) cytotoxicity guidelines found no toxicity effects at ~32μg/cm^2 using AgNP coated zirconium [47]. These studies both used direct methods for cytotoxicity. Sussman, et al. [48] also used the same method and found a dose-dependent toxicity effect in the range of 0.2–311 μg/cm^2, reaching 100% toxicity at the upper limit. However, the same study used the extract method of cytotoxicity and found no cell death within the same range [48]. Based on extraction method findings, no or little cytotoxicity is present in our coated samples. On the other hand, based on the direct method, the current concentrations are cytotoxic for acrylic and zirconium but not for based on the data available from literature.

However, the amount of AgNPs needed for in vitro studies is higher than in those needed in vivo for the same antimicrobial effect [41]. Further in vivo studies are necessary to determine the minimum concentration needed for antibacterial effects, which could potentially be lower and thus will have variable degree of cytotoxicity

The results of SEM in our study depicted a higher uniformity using spray-coating method across all three coated facial materials, which is in direct agreement reported by Butt [25], in that spray allows more adaptability, exhibits more uniform coating, and less agglomerations across different materials, particularly in specimens with regular geometry.

In this regard, Spray coating allows for deposition of AgNPs as fine, independent, aerosol microdroplets onto a surface, each containing spatially isolated aliquot of particles. Each droplet proceeds to evaporate and deposit NPs locally within an area, the size of which depends on droplet diameter and substrate wettability [21]. This provides a particle distribution mirroring the impact of droplets in a spatial pattern, independent of the dynamics of a bulk liquid film; by controlling nozzle-to-surface distance and scan speed, a macroscopically uniform coverage can be achieved without any directional or radial gradients [49]. Importantly, the absence of stabilizing polymers or surfactants, as is the case in the present study, does not allow the aggregation and clustering of NPs at an evaporating film front commonly observed with continuous liquid film, particularly in dip and spin coating of unstabilized colloidal suspensions [50].

In dip coating, the specimen being withdrawn from a NP suspension causes a thin liquid film to attach to the surface and drain with gravity confirmed by SEM finding in current study.

The movement of particles within this film is controlled by convective flux toward the receding liquid–air–solid contact line — Landau–Levich regime — is concentrating particles at the meniscus front producing a distinctive heterogeneous distribution: precisely dense particle bands or streaks in the direction of withdrawal, separated by particle-depleted regions [51,52]. When polymer binders

 doi:10.20944/preprints202605.0288.v1

or capping agents which enhance suspension viscosity and particle–substrate interactions are absent as in current study, such condition will be minimize the control the balance between particle transport and evaporation of thew solvent. This act will cause non uniform coverage that are intrinsic to the procedure rather than a consequence of parameter optimization [51]. The fact of multiple dipping cycles will occurrence will increase number of nano particles is not proper due to particles already been deposited from previous cycles on same location. That will limit the feasible uniformity despite cycle number [52].

Spin coating engages radial outward drainage of a liquid film caused by centrifugal force, causing particles accumulation at the outer edge of the spinning substrate as the film drains, producing a radial gradient in particle density —higher coverage at the periphery, lower at the center — process is enhanced due to spin speed increase and as particle size increases relative to the entrained film thickness [53]. In cases of small, flat substrates of the dimensions applied in this study, documented by Zhao and Marshall concluded that coverage uniformity about the whole substrate area for spin coating remains inferior to spray deposition [54].

Regarding the microbiological test the adhesion and direct contact tests in our study showed antimicrobial properties and are further mentioned below. However, the absence of inhibition zones in disk diffusion assay findings with all coated samples, suggests a mechanism other than ion diffusion. This result was what lead us to perform the additional and relevant direct contact test. This finding is in direct agreement with Alla, et al. [55], who reported no inhibitory zone formation around the PMMA/NP composites.

Although mixing AgNPs into PMMA is reported to have good antimicrobial activity, and a study by Galant, et al. [56] confirmed antimicrobial effects increase as AgNP concentrations and incubation times increase. However, there are implications that this approach can reduce the structural properties of the specimens. According to Galant, et al. [57] the mechanical properties of PMMA/AgNP reduce before the wt% sufficient for significant antimicrobial effect is reached. However, coating PMMA with Ag NPs creates an outer layer where particles are confined and work directly at the bacteria–material interface, having antimicrobial activity without negatively impacting the mechanical properties. This is clearly shown by Campos et al. (2017), where spray coating only 0.03 wt% AgNP concentration onto PMMA showed high antimicrobial effect against E. coli and S. aureus, and increase in flexural strength by 1.6%, concluding that surface-only approaches do not depict the same mechanical disadvantages as the bulk incorporation methods do [36].

AgNP coating of materials, particularly PMMA, is additionally more advantageous than incorporation and formation of PMMA/AgNP nanocomposites, since Ag clusters in the latter have a poor attachment to the polymeric chains and thereby result in the release of Ag NPs and ions, which can have more harmful cytotoxic effects, and less long-term efficacy [36].

The current study performed 1-hour direct contact test, and adhesion test at 1, 3, and 24 hours to compare 1- and 3-layer Ag NP spray coating of specimens.

Although a more comprehensive time-series analysis would be more informative for Ag ion release and long-term antibacterial effect, nevertheless the antimicrobial test across three time points was structured to address two clinically relevant questions simultaneously; whether an increase in the number of layers leads to a meaningful gain in surface AgNP loading and antimicrobial efficacy, and secondly, how quickly the coating affects bacteria upon contact and if this effect persists for more than 24 hours. This approach is compatible with the exploratory design stage of surface coating research focusing on antimicrobial effects where, before committing to extended protocols, the initial investigation aims for coating optimization first.

The time points chosen are relevant for the following reasons; bacteria competes with host cell for colonizing the implant within the 1st hour, which is an initially reversible adhesion, but can become irreversible through molecular bridging, tether accumulation, and cell wall deformation and lead to cell survival and proliferation despite the coating if not inhibited within 1-3 hours [13,58–60]. Liedberg and Lundeberg [61] revealed a reduction in *P. aeruginosa* adhesion within 2 hours when in contact with Ag-coated surfaces.

 doi:10.20944/preprints202605.0288.v1

Gour et al. stated that measuring early-stage adhesion at short intervals showcases the most distinguishing and sensitive window for antimicrobial activity [65]. And lastly, assessing adhesion at 24 hours is a widely used time point and has the benefit of capturing the transition from irreversible adhesion to biofilm formation [31,65].

Furthermore, there is a well-grounded rationale for comparing 1- and 3-layers. There are studies which demonstrate non-linear relation between antibacterial efficacy and amount of AgNP deposition. Lee et al. revealed that the relationship between zone of inhibition and film thickness is logarithmic; for incremental increase in antimicrobial activity, exponentially greater Ag is necessary [65]. This concept is highly relevant for clinical translatability, since additional layers may have more cost and deposition with even diminishing antibacterial effects.

One of the least standardized outcomes reported in literature is the long-term durability of silver-coated implants and orthodontic materials, where the application of different time points across the literature makes combining or comparing data through meta-analysis difficult [65,66]. The 1-hour direct contact test of our Ag-coated heat-polymerizing acrylic revealed a slight preference for 1-layer coating. This is in contrast to 1-hour adhesion test, where 3-layer had clearly more favorable antimicrobial efficacy. However, the time-series adhesion tests favored 1-layer coating of acrylic due to it's increasing efficacy across time.

This contrasts to Mukai, et al. [62], who incorporated AgNPs into heat-polymerizing PMMA, and reported no antibacterial effect in 1.5-hour adhesion test against *Streptococcus mutans*. This contrast can be due to different AgNP application, and /or the difference in bacterial species. Since it's thought that gram-negative bacteria, like *P. aeruginosa*, is more sensitive to Ag NPs than gram-positive bacteria, like *S. mutans* [63].

The study by de Castro, Valente, Agnelli, da Silva, Watanabe, Siqueira, Alves, Holtz and Dos Reis [24] concluded more *P. aeruginosa* metabolic activity in auto-polymerizing acrylic than the heat-polymerizing, thus supporting our use of heat-polymerizing acrylic.

Campos, DeAlba-Montero, Ruiz, Butrón-Téllez Girón, García-García and Loredo-Tovías [36] findings showed a stronger bacterial reduction by spray-coated acrylic than our study (99.95%). This can be attributed to the different preparation of Ag NP suspension where monomer was used rather than deionized water, and/or the smaller size of NPs. The larger specimen size can also influence this result.

Although our study showed no inhibition zones with the coating of any of the materials, a study by Haider, et al. [64], who performed spin coating of commercial Ag NPs onto PMMA, discovered inhibition zone formation against *Candida Albicans*, which increased with increasing concentration of AgNPs. Furthermore, the average inhibition zone reached at least 10 mm by 1-hour, and maintained the same inhibition size through 3-, 8-, and until 12-hours.

Silicone prosthesis can become a site for microbial accumulation due to their moisture retention and porosity, and low surrounding skin pH caused by limited patient capability [39].

In our study, silicone showed a preference for 1-layer coating in both direct contact and adhesion tests. The 1-layer coating was also more effective for the 1-, 3-, and 24 hours adhesion tests, and exhibited an increasing efficacy through time, which can be explained by Ag ion release. This is similar to a study performed by Chong, Lai, Choudhury and Amalraj [39] where the incorporation of 0.1% Ag NPs into silicone had a more sustained antimicrobial effect over 21 days on *S. aureus*. However, our 3-layered silicone exhibited a plateaued antimicrobial effect contrasting with the 0.5% AgNPs in the study, which had an initial higher efficacy in the 1st week, followed by a gradual reduction in efficacy. The authors provided a possible explanation for the reduction through the release of a burst of Ag ions from the embedded NPs at higher concentrations [39].

However, this contrasts a study performed by Choi, Jo, Han, Yoon, Lee and Yeo [37], who investigated the antimicrobial efficacy of Ag ion release and discovered the concentration needed for the aerosol-deposition coated zirconia and titanium to exhibit antibacterial effect is higher, and requires ~1,000 times the wt% used for the coating concentration in their study. This contrast can be attributed to the different innate properties between silicone and zirconium.

 doi:10.20944/preprints202605.0288.v1

The direct contact and adhesion tests of the coated zirconia had the most favorable results overall, both the single layer and 3-layer coating. However, the 3- and 24-hours adhesion tests revealed a significant decrease in antimicrobial efficacy in comparison, suggesting the involvement of factors other than the current study's investigations.

Although we achieved considerable reduction in bacterial content in the 3- and 24-hours adhesion tests compared with the uncoated zirconium, the results obtained by Choi, Jo, Han, Yoon, Lee and Yeo [37], in which aerosol deposition method was used to coat zirconia with Ag NPs, contrast our result in that the uncoated achieved less biofilm formation compared with the coated zirconia.

Zirconia by itself is thought to reduce bacterial colonization and contamination, and was further proved by absorbance values in the same study [37], therefore it seems unusual that the application of Ag coating, known for antimicrobial properties, would significantly enhance biofilm formation.

It's generally considered that various surface properties affecting bacterial growth on surfaces are surface roughness, charge, hydrophilicity, and chemical structure [65–67].

Surface roughness was significantly increased in the study [37]. However, they were not significantly higher than the 0.2 μm threshold needed for bacterial adhesion and colonization [68]. Additionally, surface roughness does not explain the initial high efficacy of zirconia followed by a relatively fast decrease in efficacy obtained in our results.

Surface charge is another factor that can explain such findings. Zirconia surface is negatively charged at the BHI broth pH = 7.4 ± 0.2, and since bacterial membranes are also negatively charged at physiological pH, colonization becomes less favorable due to electrostatic repulsion between the two surfaces [69,70]. study reports that the higher biofilm formation of the coated zirconia can be attributed to positively charged Ag ion release, neutralizing the negative charge and enhancing microbial colonization [37].

This phenomenon can explain our zirconia time-series adhesion test findings, especially because MHB broth pH = 7.3 ± 0.1 is similar to BHI broth pH [71], where the effect of both 1- and 3-layer coated zirconia was highly significant at 1-hour adhesion test, but was reduced at 3-hours, and exhibited a plateaued efficacy up to 24-hours.

The larger amount of AgNP visible on zirconia throughout the SEM images of all coating methods can be caused by innate nanorough surface topography of ceramic materials, which gives a larger functional surface area and micropore volume in comparison to PMMA and silicone, in conjunction with the coordinative and electrostatic interactions between Ag and zirconol groups on the surface [72,73]. However, in PMMA, AgNP adhesion is primarily through the weak van der Waals forces and hydrogen bonding with the carbonyl groups of the methacrylate ester and has no mechanical interlocking [74]. Silicone contrasts PMMA in that much of the NP retention occurs through physical interlocking and not chemical interactions; due to their chemical inertness, hydrophobic nature, and minor chemical functionality of the surface [75].

Silicone, being chemically inert and hydrophobic with minimal surface functionality, provides the fewest anchoring sites for AgNPs, and NP retention depends largely on mechanical entrapment rather than chemical interaction [75,76]. Silicone belonging to list of chemically inactive substrates suggests a weaker anchorage for NPs, leading to particle detachment when been subjected to environmental conditions such as salivary flow, masticatory forces, or enzymatic activity in the oral cavity. These consequences decrease the direct contact killing with time. The process of mechanical stability of particle retention under physiologically relevant conditions stated to be long-term represents a limitation of the current approach and an important direction for future consideration.

Spray coating creates uniform space of nano particle increasing bacterium placed in direct contact within the first hour incubation period, translating distributional uniformity into bactericidal efficacy disregard total silver loading. Similar findings of Seitz et al. found that spraying of NPs show optimal particle density and homogeneous distribution compared to dip coating that produce non uniform distribution. [49]. As shown in the current study, particle distribution is more effective than silver loading. However, it's necessary to mention the need for more in vitro, and in vivo and longer-

 doi:10.20944/preprints202605.0288.v1

term studies are necessary to obtain information regarding the stability, antimicrobial effects, and biocompatibility of spray-coated NPs.

Concerning the silver ion release and the direct interaction the primary antibacterial effect comes from the point where microbe directly contacts to the surface of the substrate at the contact the concentration of silver ion is much higher than the surrounding medium with make higher antimicrobial efficiency [13,77] when there is no direct contact the effect become weaker and in addition the presence of higher bacterial level even with silver ion binds to the microbial receptors reduces its effectiveness as explained by Wirth, et al. [78] presented as a factor that limits performance in the adhesion assay at the inoculum concentrations used .

Furthermore, On the matter of surface coverage factors per each material might be addressed separately. For acrylic, the current research discussed the way spray coating can produce more uniform inter-particle spacing on a smooth polymeric substrate [25,49], with reasons for the marginal performance difference between 1-layer and 3-layer coatings under direct contact that attribute to diminishing returns in coverage gain at higher particle densities rather than to additional silver loading .Considering silicone, assigned the weakness in overall performance specifically to the substrate's chemical inertness limiting particle anchorage and effective coverage density, in addition to insufficient silver quantity. For zirconia, the uniformity of early coverage did not hesitate to show the strong 1-hour performance, while the time-dependent deterioration of adhesion inhibition is attributed to Ag^+-driven charge neutralization rather than to coverage loss. Accordingly, observed differences between Adhesion and Direct Contact tests cannot be considered as an outcome of coating failure. The main cause is due to natural behavior of bacteria; hence successful coating processing has been found when bacteria is naturally deposited on surfaces. Coating malfunction occurs when bacteria is firmly been attached to the surface that leads to continuous accumulation of the bacteria causing less effect of coating in killing process. This fact leads to the expected effect of increased layers that might support the process found inconsistent freeing better performance to other aspects in current study that prevent clear judgement of specific number of layers to be favorable to a state that preferrable number of layers vary according to materials specification been used.

Therefore, the more efficacious antimicrobial activity of direct contact test in comparison to adhesion test can be explained by how the bacterial cells interact with coated surfaces. In the direct contact test, since the bacteria is directly deposited onto the coated surface and kept in proximity with the immobile AgNPs, localized dissolution of Ag^+ ions occur at concentrations much higher than is measurable in the bulk medium, leading to bactericidal action via a direct contact mechanism [13]. Thus, physical separation of bacteria from the coated surface substantially reduces antimicrobial effects, since the Ag^+ release directly at NP–cell contact point has much more toxicity than dissolved Ag ions and therefore is dependent on the interface rather than freely diffusing ions [77].

This contrasts adhesion assays where the cells approach freely to the surface and are not forced into persistent contact with the surface Ag NPs. Additionally, the higher inoculum load and the competitive binding of Ag ions to cell biomass and extracellular products can reduce Ag^+ concentrations available for bactericidal action [77].

These mechanisms give a clear explanation not only for why direct contact has higher antibacterial efficacy, but also the reason why spray coating is preferable for antimicrobial action; due to their uniform NP distribution.

Additionally, two critical implications for clinical use can be anticipated through these mechanisms. The first being durability. The coatings that depend on ion release will eventually lead to lower antimicrobial levels, as there are only finite amounts of Ag and consistent ion diffusion will reduce this reservoir [79]. This limitation, however, is subsided in coatings with direct contact killings in which the operation remains below the bulk diffusion. This is true as long as NPs remain adherent to the surface; since the killings will occur with direct contact and the mass and reactive surface area of the particles are maintained. Therefore, such coatings are expected to preserve the antimicrobial qualities for much longer durations than that diffusion-dependent system at equivalent silver loading

 doi:10.20944/preprints202605.0288.v1

[13]. Secondly, due to the fact that the primary route of cytotoxicity—Ag ion release—is avoided, the coatings are likely to have an enhanced biocompatibility profile with preserved contact-killing action.

Acknowledgement should be given that the durability of the coatings is dependent on the quality and longevity of NP adherence. The current study used only deionized water suspension without capping agents or polymer binders, depending mainly on physical adsorption for NP attachment. Although the absence of additive agents remove the possibility of introducing potentially cytotoxic materials, these additives provide covalent immobilization methods, which are improvements for NP stability and persistent antimicrobial effect when compared with the weaker anchor the physical adsorption provides [80]. Recently, alternative systems such as gallium (Ga) and silver–gallium (Ag–Ga) have gained attention. Unlike silver, gallium acts by disrupting bacterial iron metabolism, as it mimics Fe^{3+} but cannot participate in redox reactions, thereby inhibiting essential cellular processes. While in current study the main focus was to provide more practical and not changing the surface property like the surface gallium. This different mechanism, along with the potential for more controlled ion release, makes Ga-based systems promising candidates for future applications [81].

Finally, Current study was designed on this principle. Direct cytocompatibility testing against primary oral mucosal cells under conditions representative of prosthetic use has not been performed in this study and is identified as a necessary and clearly defined direction for future work.

5. Conclusions

The findings in our study reveal a more uniform distribution of Ag NPs via spray coating technique than spin or dip coatings via SEM. The antimicrobial efficacy of the relatively low commercial NP concentration was effective against *P. aeruginosa* on all three facial prosthetic materials, and the efficacy varied depending on the number of sprays and layers, the material type, different types of antimicrobial tests, and their time-dependent variables.

FTIR revealed no chemical modifications of the substrates, whilst EDS proved an effective Ag NP deposition, preserving the innate material qualities.

Disk diffusion test had no inhibition zones, and direct contact tests revealed significantly higher antibacterial efficacy than adhesion test, indicating a more contact-dependent action rather than diffusion-based for coated surfaces.

Time-dependent adhesion tests against *P. aeruginosa* showed a reduced bacterial content for coated surfaces when compared with uncoated ones. The findings were dependent on the number of coating layers, where 1-layer outperformed 3-layers, suggesting an increase in the amount of Ag NP does not necessarily equate with an increase in its antibacterial efficiency. The material performance of coated acrylic and silicone exhibited a constantly increasing reduction in bacterial adhesion across time points, whilst zirconium showed the contrary.

The approach utilized in this study shows preliminary relevance for clinical applications due to the ease of implementation, potentially enabling the development of biocompatible, long-term dental and maxillofacial prosthesis in high-risk microbial environments.

This study is not without limitations however, and various other longer-term and additional in vitro antimicrobial investigations against *P. aeruginosa* and other microbial species, in vivo animal and human studies, and mechanical and cytotoxicity studies are required for ensuring possible future applications.

Author Contributions: Conceptualization, Z.D.O.M. and L.A.A. and W.M.D.; methodology, W.M.D. and L.A.A.; software, W.M.D; validation, L.A.A. and W.M.D.; formal analysis, W.M.D.; investigation, W.M.D. and L.A.A.; resources, L.A.A.; data curation, L.A.A. and W.M.D.; writing—original draft preparation, W.M.D.; writing—review and editing, W.M.D. and Z.D.O.M.; visualization, W.M.D; supervision, Z.D.O.M. and L.A.A.; project administration, L.A.A. and W.M.D.; funding acquisition, W.M.D. All authors have read and agreed to the published version of the manuscript.

Funding: This research received no external funding.

 doi:10.20944/preprints202605.0288.v1

Institutional Review Board Statement: Not applicable.

Informed Consent Statement: Not applicable.

Data Availability Statement: Dataset available on request from the authors.

Acknowledgments: The authors would like to thank Anas Mtawea Alhusban for helping with the equipment and data acquisition of the coating method investigations and characterization tests during experimental work. Special thanks to Qutaiba Omar Ababneh, for providing the opportunity to perform the investigations in the laboratory, and Ms. Ekhlas Hashem Al-Rousan for her help with the technical assistance for the microbiological methodology of the study. The principal authors also extends their deepest appreciations to their father, Mand Ibrahim Dizayee, for his help with statistical analysis, and Ahmed Dilshad Rostum, for his assistance in refining the English language and style of this manuscript.

Conflicts of Interest: The authors declare no conflicts of interest.

Abbreviations

The following abbreviations are used in this manuscript:

PMMA	Polymethyl Methacrylate
CAD/CAM	Computer-aided design/computer-aided manufacturing
NP	Nanoparticle
CNC	Computer Numerical Control
FESEM	Field Emission Scanning Electron Microscope
MIC	Minimal inhibitory concentration
MBC	Minimal Bactericidal Concentration
DLS	Dynamic Light Scattering
SEM	Scanning Electron Microscope
FTIR	Fourier Transform Infrared Spectroscopy
NIR	Near-Infrared
ATR	Attenuated Total Reflectance
EDS	Energy Dispersive X-ray Spectroscopy
EDXRF	Energy Dispersive X-Ray Fluorescence

Appendix A

Appendix A.1

Table A1. General materials and devices used.

Materials used	Device Details
CNC Machine	Shandong, Z1313 CNC Machine, China
CAD/CAM milling machine	DWX-52Di, DG SHAPE, Japan
Furnace	Programat S1 1600, Ivoclar Vivadent
Type 3 dental stone	Whip Mix Corp., USA
C-silicone liner	Bonasil, BMS Dental, Italy
FESEM	Inspect F50, FEI Company, Hillsboro, OR, USA
Sputter Coater (Platinum)	Emitech K550X Quorum Technologies Ltd., Laughton, UK
Sputter Coater (Gold)	Q150R ES Plus, Quorum Technologies Ltd., Laughton, UK
Type I ultrapure water	Milli-Q, Merck Millipore, Germany
Probe sonicator	Sonics & Materials, Vibra-Cell VCX130, USA
UV-Visible Spectrophotometer	BioMate 3, Thermo Scientific, USA
Vortex mixer	Vortex-Genie, VWR International, USA
Plate shaker	PST-60HL, BioSan, Latvia
Zetasizer	Nano ZS90, Malvern Panalytical, UK

 doi:10.20944/preprints202605.0288.v1

UV–Vis–NIR Spectrophotometry	Agilent Technologies, Cary 5000 UV-Vis-NIR, USA
3D stereomicroscope	KRUSS, German
High-frequency generator (plasma treatment)	BD-20V, Electro-Technic Products, US
Water bath shaker	Grant OLS Aqua Pro, Grant Instruments, UK

Appendix A.2

Table A2. Details of the silver nanoparticles used.

	Parameter	Specification/Detail
Trade Name / Source	Silver Nanoparticles	US Research Nanomaterials, Inc. (Houston, TX, USA)
Manufacturing Method	Atomization	Electric high-temperature and high-pressure air flow (US1038)
Chemical Purity	Silver (Ag) basis	99.99%
Morphology	Particle Shape / Color	Spherical / Black
Particle Size	Average Diameter	20nm
Size Distribution	Range	80% at 20 nm; 10% < 20 nm; 10% > 20 nm 2-3% reaching 70nm
Surface Area	Specific Surface Area (SSA)	18–22m^2 / g
Density	True Density	10.5g / cm^3

Appendix B

Appendix B.1

Table 1. Microbiological material and procedural details.

Parameters	Specifications
Microorganism	*P. aeruginosa* (ATCC 27853)
Retrieval	Frozen culture vials stored at -80 °C
Culture Media used	Mueller-Hinton agar & broth
Biological Safety Cabinet (BSC)	ESCO Airstream® Class II BSC
Laboratory Freezer	BIOBASE, China
Incubator	IN plus, Memmert, Germany
Mueller-Hinton Broth powder	Condalab, Conda Labs, Spain, Catalog number: 2140
Autoclave	JLab Tech, China
Microbial suspension preparation / Optical Density	0.5 McFarland standard (1 × 108) CFU/ mL) Range: 0.08-0.13 at 625 nm
Sterilization	Autoclave: 121 °C for 20 minutes

Table 2. The complete sample size used for this study.

Tests	Materials	Condition	Replicates	Per material (n)	Total (n)
SEM	Ac, Si, Zr	Spray, Spin, Dip, Uncoated	1	4	12
Spray numbers	Zr only	5,10,15 sprays	1	-	3
Adhesion 1 hour	Ac, Si, Zr	Uncoated, 1L, 3L coated	3	9	27
Direct contact 1 hour	Ac, Si, Zr	Uncoated, 1L, 3L coated	3	9	27
Agar diffusion	Ac, Si, Zr	Uncoated, 1L, 3L coated	1	3	9
Adhesion 1-, 3-, 24-hour(s)	Ac, Si, Zr	Uncoated, 1L, 3L coated	1	9	27
FTIR	Ac, Si, Zr	Uncoated, 1L coated	1	1	6

 doi:10.20944/preprints202605.0288.v1

EDS	Ac, Si, Zr	Uncoated, 1L coated	1	1	6
EDXRF	Ac, Si, Zr	Uncoated, 1L coated	1	1	6

References

1. Natarajan, P.; Kumar, S.M.; Natarajan, S.; Sridharan, K.; Kalkura, S.N. Nano-particle coated or impregnated acrylic resins in dental applications: A systematic review of in Vivo Evidence on mechanical properties, biocompatibility and clinical performance. *Journal of Oral Biology and Craniofacial Research* **2025**, *15*, 1190-1199.
2. Kumar, A.; Seenivasan, M.K.; Inbarajan, A. A literature review on biofilm formation on silicone and poymethyl methacrylate used for maxillofacial prostheses. *Cureus* **2021**, *13*.
3. Gligorijević, N.; Mihajlov-Krstev, T.; Kostić, M.; Nikolić, L.; Stanković, N.; Nikolić, V.; Dinić, A.; Igić, M.; Bernstein, N. Antimicrobial properties of silver-modified denture base resins. *Nanomaterials* **2022**, *12*, 2453.
4. Kauke-Navarro, M.; Knoedler, L.; Knoedler, S.; Deniz, C.; Stucki, L.; Safi, A.-F. Balancing beauty and science: a review of facial implant materials in craniofacial surgery. *Frontiers in Surgery* **2024**, *11*, 1348140.
5. Srimaneepong, V.; Heboyan, A.; Zafar, M.S.; Khurshid, Z.; Marya, A.; Fernandes, G.V.; Rokaya, D. Fixed prosthetic restorations and periodontal health: a narrative review. *Journal of functional biomaterials* **2022**, *13*, 15.
6. Robu, A.; Antoniac, A.; Grosu, E.; Vasile, E.; Raiciu, A.D.; Iordache, F.; Antoniac, V.I.; Rau, J.V.; Yankova, V.G.; Ditu, L.M. Additives imparting antimicrobial properties to acrylic bone cements. *Materials* **2021**, *14*, 7031.
7. Costa, R.T.F.; Pellizzer, E.P.; Vasconcelos, B.C.d.E.; Gomes, J.M.L.; Lemos, C.A.A.; de Moraes, S.L.D. Surface roughness of acrylic resins used for denture base after chemical disinfection: A systematic review and meta-analysis. *Gerodontology* **2021**, *38*, 242-251.
8. Ferro, A.C.; Spavieri, J.H.P.; Ribas, B.R.; Scabelo, L.; Jorge, J.H. Do denture cleansers influence the surface roughness and adhesion and biofilm formation of Candida albicans on acrylic resin? Systematic review and meta-analysis. *Journal of Prosthodontic Research* **2023**, *67*, 164-172.
9. Parcheta, M.; Sobiesiak, M. Preparation and functionalization of polymers with antibacterial properties—Review of the recent developments. *Materials* **2023**, *16*, 4411.
10. Arora, S.; Jain, J.; Rajwade, J.; Paknikar, K. Cellular responses induced by silver nanoparticles: in vitro studies. *Toxicol. Lett.* **2008**, *179*, 93-100.
11. Greulich, C.; Braun, D.; Peetsch, A.; Diendorf, J.; Siebers, B.; Epple, M.; Köller, M. The toxic effect of silver ions and silver nanoparticles towards bacteria and human cells occurs in the same concentration range. *RSC advances* **2012**, *2*, 6981-6987.
12. Shayo, G.M.; Elimbinzi, E.; Shao, G.N. Preparation methods, applications, toxicity and mechanisms of silver nanoparticles as bactericidal agent and superiority of green synthesis method. *Heliyon* **2024**, *10*, doi:10.1016/j.heliyon.2024.e36539.
13. Agnihotri, S.; Mukherji, S.; Mukherji, S. Immobilized silver nanoparticles enhance contact killing and show highest efficacy: elucidation of the mechanism of bactericidal action of silver. *Nanoscale* **2013**, *5*, 7328-7340, doi:10.1039/C3NR00024A.
14. Dhaka, A.; Mali, S.C.; Sharma, S.; Trivedi, R. A review on biological synthesis of silver nanoparticles and their potential applications. *Results in Chemistry* **2023**, *6*, 101108.
15. Abbas, R.; Luo, J.; Qi, X.; Naz, A.; Khan, I.A.; Liu, H.; Yu, S.; Wei, J. Silver Nanoparticles: Synthesis, Structure, Properties and Applications. *Nanomaterials* **2024**, *14*, 1425.
16. Murray, C.J.L.; Ikuta, K.S.; Sharara, F.; Swetschinski, L.; Robles Aguilar, G.; Gray, A.; Han, C.; Bisignano, C.; Rao, P.; Wool, E.; et al. Global burden of bacterial antimicrobial resistance in 2019: a systematic analysis. *The Lancet* **2022**, *399*, 629-655, doi:10.1016/S0140-6736(21)02724-0.
17. Organization, W.H. WHO publishes list of bacteria for which new antibiotics are urgently needed. Available online: https://www.who.int/en/news-room/detail/27-02-2017-who-publishes-list-of-bacteria-for-which-new-antibiotics-are-urgently-needed (accessed on
18. Dube, E.; Okuthe, G.E. Silver Nanoparticle-Based Antimicrobial Coatings: Sustainable Strategies for Microbial Contamination Control. *Microbiol. Res. (Pavia)* **2025**, *16*, 110.

 doi:10.20944/preprints202605.0288.v1

19. Harun-Ur-Rashid, M.; Foyez, T.; Krishna, S.B.N.; Poda, S.; Imran, A.B. Recent advances of silver nanoparticle-based polymer nanocomposites for biomedical applications. *RSC Advances* **2025**, *15*, 8480-8505, doi:10.1039/D4RA08220F.
20. Tran, D.-T.; Chen, F.-H.; Wu, G.-L.; Ching, P.C.O.; Yeh, M.-L. Influence of Spin Coating and Dip Coating with Gelatin/Hydroxyapatite for Bioresorbable Mg Alloy Orthopedic Implants: In Vitro and In Vivo Studies. *ACS Biomaterials Science & Engineering* **2023**, *9*, 705-718, doi:10.1021/acsbiomaterials.2c01122.
21. Yang, R.; Mazalan, E.; Chaudhary, K.T.; Haider, Z.; Ali, J. Non-vacuum deposition methods for thin film solar cell: Review. *AIP Conf. Proc.* **2017**, *1824*, doi:10.1063/1.4978836.
22. Marassi, V.; Di Cristo, L.; Smith, S.G.J.; Ortelli, S.; Blosi, M.; Costa, A.L.; Reschiglian, P.; Volkov, Y.; Prina-Mello, A. Silver nanoparticles as a medical device in healthcare settings: a five-step approach for candidate screening of coating agents. *Royal Society Open Science* **2018**, *5*, doi:10.1098/rsos.171113.
23. Wiegand, I.; Hilpert, K.; Hancock, R.E. Agar and broth dilution methods to determine the minimal inhibitory concentration (MIC) of antimicrobial substances. *Nat. Protoc.* **2008**, *3*, 163-175.
24. de Castro, D.T.; Valente, M.L.; Agnelli, J.A.M.; da Silva, C.H.L.; Watanabe, E.; Siqueira, R.L.; Alves, O.L.; Holtz, R.D.; Dos Reis, A.C. In vitro study of the antibacterial properties and impact strength of dental acrylic resins modified with a nanomaterial. *The Journal of prosthetic dentistry* **2016**, *115*, 238-246.
25. Butt, M.A. Thin-Film Coating Methods: A Successful Marriage of High-Quality and Cost-Effectiveness—A Brief Exploration. *Coatings* **2022**, *12*, 1115.
26. Tada, A.; Hanada, N. Opportunistic respiratory pathogens in the oral cavity of the elderly. *FEMS Immunol. Med. Microbiol.* **2010**, *60*, 1-17, doi:10.1111/j.1574-695X.2010.00709.x.
27. Murthy, S.K.; Baltch, A.L.; Smith, R.P.; Desjardin, E.K.; Hammer, M.C.; Conroy, J.V.; Michelsen, P.B. Oropharyngeal and fecal carriage of Pseudomonas aeruginosa in hospital patients. *J. Clin. Microbiol.* **1989**, *27*, 35-40, doi:doi:10.1128/jcm.27.1.35-40.1989.
28. Botzenhart, K.; Puhr, O.F.; Döring, G. [Pseudomonas aeruginosa in the oral cavity: occurrence and age distribution of adult germ carriers]. *Zentralblatt fur Bakteriologie, Mikrobiologie und Hygiene. 1. Abt. Originale B, Hygiene* **1985**, *180 5-6*, 471-479.
29. Leibovitz, A.; Dan, M.; Zinger, J.; Carmeli, Y.; Habot, B.; Segal, R. Pseudomonas aeruginosa and the oropharyngeal ecosystem of tube-fed patients. *Emerging infectious diseases* **2003**, *9*, 956.
30. Tada, A. The relation between tube feeding and Pseudomonas aeruginosa detection in the oral cavity. *J. Gerontol. A Biol. Sci. Med. Sci.* **2002**, *57*, M71.
31. O'Donnell, L.E.; Smith, K.; Williams, C.; Nile, C.J.; Lappin, D.F.; Bradshaw, D.; Lambert, M.; Robertson, D.P.; Bagg, J.; Hannah, V. Dentures are a reservoir for respiratory pathogens. *Journal of prosthodontics* **2016**, *25*, 99-104.
32. Lim, T.W.; Li, K.Y.; Burrow, M.F.; McGrath, C. Prevalence of respiratory pathogens colonizing on removable dental prostheses in healthy older adults: A systematic review and meta-analysis. *Journal of Prosthodontics* **2024**, *33*, 417-426.
33. Jones, C.J.; Grotewold, N.; Wozniak, D.J.; Gloag, E.S. Pseudomonas aeruginosa Initiates a Rapid and Specific Transcriptional Response during Surface Attachment. *J. Bacteriol.* **2022**, *204*, e00086-00022, doi:doi:10.1128/jb.00086-22.
34. Silva, M.E.P.d.; Suica, L.M.d.M.; Rodrigues, R.S.; Ramos, I.V.G.; Carvalho, A.G.; Silva Lima, N.C.d.; Belém, M.G.L.; Esquerdo, R.P.; Matos, N.B. Oral cavity colonization by Pseudomonas aeruginosa in patients admitted in the intensive care units (ICUs). *Brazilian Journal of Oral Sciences* **2025**, *24*, e257686, doi:10.20396/bjos.v24i00.8677686.
35. Behbehani, M.; McDonald, A.; Nair, S.P.; Green, I.M. Susceptibility of Pseudomonas aeruginosa and Acinetobacter baumannii biofilms grown on denture acrylic to denture-cleaning agents and sonication. *bioRxiv* **2022**, 2022.2009.2021.508680, doi:10.1101/2022.09.21.508680.
36. Campos, V.; DeAlba-Montero, I.; Ruiz, F.; Butrón-Téllez Girón, C.; García-García, E.; Loredo-Tovías, M. Simple and rapid method for silver nanoparticles incorporation in polymethyl methacrylate (PMMA) substrates. *Superficies y vacío* **2017**, *30*, 51-55.

 doi:10.20944/preprints202605.0288.v1

37. Choi, S.; Jo, Y.-H.; Han, J.-S.; Yoon, H.-I.; Lee, J.-H.; Yeo, I.-S.L. Antibacterial activity and biocompatibility of silver coating via aerosol deposition on titanium and zirconia surfaces. *International Journal of Implant Dentistry* **2023**, *9*, 24.
38. Qing, Y.a.; Cheng, L.; Li, R.; Liu, G.; Zhang, Y.; Tang, X.; Wang, J.; Liu, H.; Qin, Y. Potential antibacterial mechanism of silver nanoparticles and the optimization of orthopedic implants by advanced modification technologies. *International journal of nanomedicine* **2018**, 3311-3327.
39. Chong, W.X.; Lai, Y.X.; Choudhury, M.; Amalraj, F.D. Efficacy of incorporating silver nanoparticles into maxillofacial silicone against Staphylococcus aureus, Candida albicans, and polymicrobial biofilms. *The Journal of Prosthetic Dentistry* **2022**, *128*, 1114-1120.
40. Alhosani, F.; Islayem, D.; Almansoori, S.; Zaka, A.; Nayfeh, L.; Rezk, A.; Yousef, A.F.; Pappa, A.M.; Nayfeh, A. Antibiofilm activity of ZnO–Ag nanoparticles against Pseudomonas aeruginosa. *Sci. Rep.* **2025**, *15*, 17321.
41. Tabassum, N.; Khan, F.; Jeong, G.-J.; Jo, D.-M.; Kim, Y.-M. Silver nanoparticles synthesized from Pseudomonas aeruginosa pyoverdine: Antibiofilm and antivirulence agents. *Biofilm* **2024**, *7*, 100192, doi:https://doi.org/10.1016/j.bioflm.2024.100192.
42. Gao, X.; Johnson, W.E.; Yourick, M.R.; Campasino, K.; Sprando, R.L.; Yourick, J.J. Hepatotoxicity of silver nanoparticles: Benchmark concentration modeling of an in vitro transcriptomics study in human iPSC-derived hepatocytes. *Regulatory Toxicology and Pharmacology* **2024**, *151*, 105653, doi:https://doi.org/10.1016/j.yrtph.2024.105653.
43. Tijana, A.; Valentina, V.; Nataša, T.; Miloš, H.-M.; Suzana, G.A.; Milica, B.; Yoshiyuki, H.; Hironori, S.; Ivanič, A.; Rebeka, R. Mechanical properties of new denture base material modified with gold nanoparticles. *Journal of prosthodontic research* **2021**, *65*, 155-161.
44. Rukiqi, G.; Shala, K.; Pustina, T.; Aliaj, F.; Musliu, E.; Lushaj, M. Hardness and Density of Conventional and Monolithic Zirconia after Sintering.
45. Liu, Q.; Shao, L.; Xiang, H.; Zhen, D.; Zhao, N.; Yang, S.; Zhang, X.; Xu, J. Biomechanical characterization of a low density silicone elastomer filled with hollow microspheres for maxillofacial prostheses. *J. Biomater. Sci. Polym. Ed.* **2013**, *24*, 1378-1390.
46. Agarwal, A.; Weis, T.L.; Schurr, M.J.; Faith, N.G.; Czuprynski, C.J.; McAnulty, J.F.; Murphy, C.J.; Abbott, N.L. Surfaces modified with nanometer-thick silver-impregnated polymeric films that kill bacteria but support growth of mammalian cells. *Biomaterials* **2010**, *31*, 680-690.
47. Yamada, R.; Nozaki, K.; Horiuchi, N.; Yamashita, K.; Nemoto, R.; Miura, H.; Nagai, A. Ag nanoparticle–coated zirconia for antibacterial prosthesis. *Materials Science and Engineering: C* **2017**, *78*, 1054-1060.
48. Sussman, E.M.; Casey, B.J.; Dutta, D.; Dair, B.J. Different cytotoxicity responses to antimicrobial nanosilver coatings when comparing extract-based and direct-contact assays. *J. Appl. Toxicol.* **2015**, *35*, 631-639.
49. Seitz, B.S.; Plenagl, N.; Raschpichler, M.; Vögeling, H.; Wojcik, M.; Pinnapireddy, S.R.; Brüßler, J.; Bakowsky, U. Nanoparticles and liposomes for the surface modification of implants: a comparative study of spraying and dipping techniques. *physica status solidi (a)* **2018**, *215*, 1700847.
50. Jeong, W.; Lee, H.; Hwang, Y.J.; An, B.; Lee, Y.; Jeong, H.; Kim, G.; Park, Y.; Kim, M.; Ha, D.-H. Solution processing for colloidal nanoparticle thin film: From fundamentals to applications. *Advances in colloid and interface science* **2025**, *342*, 103538.
51. Gans, A.; Dressaire, E.; Colnet, B.; Saingier, G.; Bazant, M.Z.; Sauret, A. Dip-coating of suspensions. *Soft matter* **2019**, *15*, 252-261.
52. Palma, S.; Lhuissier, H. Dip-coating with a particulate suspension. *J. Fluid Mech.* **2019**, *869*, R3.
53. Scriven, L. Physics and applications of dip coating and spin coating. *MRS Online Proceedings Library* **1988**, *121*, 717-729.
54. Zhao, Y.; Marshall, J. Spin coating of a colloidal suspension. *Phys. Fluids* **2008**, *20*.
55. Alla, R.K.; Guduri, V.; Kandi, V.; Swamy, K.N.; Vyas, R.; Guddala, N. Evaluation of the antimicrobial activity of heat-cure denture base resin materials incorporated with silver nanoparticles. *International Journal of Dental Materials* **2019**, *01*, 40-47, doi:10.37983/IJDM.2019.1201.
56. Galant, K.; Podziewska, M.; Chęciński, M.; Chęcińska, K.; Turosz, N.; Chlubek, D.; Korcz, T.; Sikora, M. The Effect of Silver Nanoparticle Addition on the Antimicrobial Properties of Poly(methyl methacrylate) Used for Fabrication of Dental Appliances: A Systematic Review. *Int. J. Mol. Sci.* **2025**, *26*, 11633.

 doi:10.20944/preprints202605.0288.v1

57. Galant, K.; Turosz, N.; Chęcińska, K.; Chęciński, M.; Cholewa-Kowalska, K.; Karwan, S.; Chlubek, D.; Sikora, M. Silver Nanoparticles (AgNPs) Incorporation into Polymethyl Methacrylate (PMMA) for Dental Appliance Fabrication: A Systematic Review and Meta-Analysis of Mechanical Properties. *Int. J. Mol. Sci.* **2024**, *25*, 12645.
58. Wassall, M.A.; Santin, M.; Isalberti, C.; Cannas, M.; Denyer, S.P. Adhesion of bacteria to stainless steel and silver-coated orthopedic external fixation pins. *J. Biomed. Mater. Res.* **1997**, *36*, 325-330, doi:https://doi.org/10.1002/(SICI)1097-4636(19970905)36:3<325::AID-JBM7>3.0.CO;2-G.
59. An, Y.H.; Friedman, R.J. Concise review of mechanisms of bacterial adhesion to biomaterial surfaces. *J. Biomed. Mater. Res.* **1998**, *43*, 338-348.
60. Carniello, V.; Peterson, B.W.; van der Mei, H.C.; Busscher, H.J. Physico-chemistry from initial bacterial adhesion to surface-programmed biofilm growth. *Advances in Colloid and Interface Science* **2018**, *261*, 1-14, doi:https://doi.org/10.1016/j.cis.2018.10.005.
61. Liedberg, H.; Lundeberg, T. Silver coating of urinary catheters prevents adherence and growth of Pseudomonas aeruginosa. *Urol. Res.* **1989**, *17*, 357-358, doi:10.1007/BF00510525.
62. Mukai, M.-K.; Iegami, C.-M.; Cai, S.; Stegun, R.-C.; Galhardo, A.-P.-M.; Costa, B. Antimicrobial effect of silver nanoparticles on polypropylene and acrylic resin denture bases. *Journal of Clinical and Experimental Dentistry* **2023**, *15*, e38.
63. Dakal, T.C.; Kumar, A.; Majumdar, R.S.; Yadav, V. Mechanistic Basis of Antimicrobial Actions of Silver Nanoparticles. *Front. Microbiol.* **2016**, *Volume 7—2016*, doi:10.3389/fmicb.2016.01831.
64. Haider, B.; Imran, M.; Raza, M.; Riaz, Z.; Hanif, A.; Akram, S. Antifungal Effect of Silver Nano Particles Coating on Denture Base Specimens Made of Acrylic Resin. *Journal of the Pakistan Dental Association* **2022**, *31*.
65. Zheng, S.; Bawazir, M.; Dhall, A.; Kim, H.-E.; He, L.; Heo, J.; Hwang, G. Implication of Surface Properties, Bacterial Motility, and Hydrodynamic Conditions on Bacterial Surface Sensing and Their Initial Adhesion. *Frontiers in Bioengineering and Biotechnology* **2021**, *Volume 9—2021*, doi:10.3389/fbioe.2021.643722.
66. Song, F.; Koo, H.; Ren, D. Effects of material properties on bacterial adhesion and biofilm formation. *J. Dent. Res.* **2015**, *94*, 1027-1034.
67. Kreve, S.; Reis, A.C.D. Bacterial adhesion to biomaterials: What regulates this attachment? A review. *Jpn. Dent. Sci. Rev.* **2021**, *57*, 85-96, doi:https://doi.org/10.1016/j.jdsr.2021.05.003.
68. Bollenl, C.M.; Lambrechts, P.; Quirynen, M. Comparison of surface roughness of oral hard materials to the threshold surface roughness for bacterial plaque retention: a review of the literature. *Dent. Mater.* **1997**, *13*, 258-269.
69. Berne, C.; Ellison, C.K.; Ducret, A.; Brun, Y.V. Bacterial adhesion at the single-cell level. *Nature Reviews Microbiology* **2018**, *16*, 616-627.
70. Oh, Y.J.; Khan, E.S.; Campo, A.d.; Hinterdorfer, P.; Li, B. Nanoscale Characteristics and Antimicrobial Properties of (SI-ATRP)-Seeded Polymer Brush Surfaces. *ACS Applied Materials & Interfaces* **2019**, *11*, 29312-29319, doi:10.1021/acsami.9b09885.
71. Condalab. *Mueller–Hinton Broth Technical Data Sheet*; Condalab: Madrid, Spain, 2021.
72. Iqbal, M.N.; Shen, Z.J.; Bengtsson, T.; Eriksson, M. Surface Effect of Nano-Roughened Yttria-Doped Zirconia on Salivary Protein Adhesion. *Materials* **2021**, *14*, 6412.
73. Liu, T.; Li, Y.; Liang, C. The adsorption and growth of Ag n (n= 1–4) clusters on cubic, monoclinic, and tetragonal ZrO 2 surfaces: a first-principles study. *New J. Chem.* **2020**, *44*, 2268-2274.
74. Borse, S.; Temgire, M.; Khan, A.; Joshi, S. Photochemically assisted one-pot synthesis of PMMA embedded silver nanoparticles: Antibacterial efficacy and water treatment. *RSC advances* **2016**, *6*, 56674-56683.
75. Bovero, E.; Magee, K.E.; Young, E.C.; Menon, C. Dispersion of silver nanoparticles into polymer matrix dry adhesives to achieve antibacterial properties, increased adhesion, and optical absorption. *Macromolecular Reaction Engineering* **2013**, *7*, 624-631.
76. Victor, S.-U.; Regina, C.Y.; Roberto, V.-B.J. Immobilization of gold and silver on a biocompatible porous silicone matrix to obtain hybrid nanostructures. *J. Biomater. Nanobiotechnol.* **2018**, *9*, 41-50.
77. Bondarenko, O.; Ivask, A.; Käkinen, A.; Kurvet, I.; Kahru, A. Particle-cell contact enhances antibacterial activity of silver nanoparticles. *PLoS One* **2013**, *8*, e64060.

 doi:10.20944/preprints202605.0288.v1

78. Wirth, S.M.; Bertuccio, A.J.; Cao, F.; Lowry, G.V.; Tilton, R.D. Inhibition of bacterial surface colonization by immobilized silver nanoparticles depends critically on the planktonic bacterial concentration. *Journal of Colloid and Interface Science* **2016**, *467*, 17-27, doi:https://doi.org/10.1016/j.jcis.2015.12.049.
79. Li, Z.; Lee, D.; Sheng, X.; Cohen, R.E.; Rubner, M.F. Two-level antibacterial coating with both release-killing and contact-killing capabilities. *Langmuir* **2006**, *22*, 9820-9823.
80. Ghilini, F.; Rodríguez González, M.C.; Minan, A.G.; Pissinis, D.; Creus, A.H.; Salvarezza, R.C.; Schilardi, P.L. Highly stabilized nanoparticles on poly-L-lysine-coated oxidized metals: a versatile platform with enhanced antimicrobial activity. *ACS applied materials & interfaces* **2018**, *10*, 23657-23666.
81. Qiao, Y.; Li, Y.; Ye, Y.; Yu, Y.; Wang, W.; Yao, K.; Zhou, M. Gallium-Based Nanoplatform for Combating Multidrug-Resistant Pseudomonas aeruginosa and Postoperative Inflammation in Endophthalmitis Secondary to Cataract Surgery. *ACS Applied Materials & Interfaces* **2022**, *14*, 51763-51775, doi:10.1021/acsami.2c15834.